

# Table of Contents

<b>1</b>	<b>Introduction</b>	<b>1</b>
<b>2</b>	<b>Literature Review</b>	<b>5</b>
<b>3</b>	<b>Aims and Objectives</b>	<b>8</b>
3.1	Primary Aims . . . . .	8
<b>4</b>	<b>Methodology</b>	<b>10</b>
4.1	Google Colab Platform . . . . .	10
4.1.1	Python and PyTorch Framework . . . . .	10
4.2	Dataset Preparation and Refinement . . . . .	11
4.2.1	Stage 1: Initial Dataset Collection . . . . .	11
4.2.2	Stage 2: Refined Dataset - Focus on Adult In-flight Images . . . . .	11
4.2.3	Stage 3: High-Quality Dataset . . . . .	12
4.3	Debugging and Iterative Development Methodology . . . . .	12
4.3.1	Pipeline Validation and Early Debugging . . . . .	12
4.4	Transfer Learning Approach . . . . .	13
4.4.1	Common Implementation Strategy . . . . .	14
4.4.2	Data Preparation and Augmentation . . . . .	14
4.4.3	Image Preprocessing . . . . .	15
4.4.4	Training Optimization Strategy . . . . .	15
4.4.5	Regularization Techniques . . . . .	16
4.4.6	Addressing Class Imbalance . . . . .	16
4.4.7	Dataset Management . . . . .	17
4.4.8	Evaluation Strategy . . . . .	17
4.4.9	Model Checkpointing and Evaluation . . . . .	18
4.5	Model Architectures and Specific Implementations . . . . .	18
4.5.1	VGG-16 Architecture . . . . .	18

4.5.2	Vision Transformer (ViT) Architecture . . . . .	20
4.5.3	ViT for Fine-Grained Classification . . . . .	20
4.5.4	Inception v3 Architecture . . . . .	22
4.5.5	Residual Network (ResNet-50) Implementation . . . . .	23
4.5.6	Custom CNN with Squeeze-and-Excitation Blocks . . . . .	24
4.6	Model Interpretability Methodologies . . . . .	25
4.6.1	Gradient-weighted Class Activation Mapping (Grad-CAM) . . . . .	25
4.6.2	Attention Rollout for Vision Transformers . . . . .	26
4.6.3	Grad-CAM for Vision Transformers . . . . .	27
4.6.4	Enhanced ViT Implementation . . . . .	28
4.6.5	Interpretable ViT Implementation . . . . .	28
4.6.6	Comparison Framework . . . . .	29
.1	Additional Interpretability Techniques . . . . .	29
.1.1	DeepLIFT . . . . .	30
.1.2	Saliency Maps . . . . .	30
.1.3	Integrated Gradients for Vision Transformers . . . . .	30
.1.4	Guided Backpropagation for Vision Transformers . . . . .	31
.1.5	Conclusion on Additional Methods . . . . .	31
.2	Feature Analysis and Interpretability for Fine-Grained Gull Classification	32
.2.1	Methodology for Wing and Wingtip Intensity Analysis . . . . .	32
.3	Local Binary Pattern Implementation for Seagull Species Analysis . . . . .	34
.3.1	Introduction to Local Binary Patterns . . . . .	34
.3.2	Implementation Methodology . . . . .	35
.3.3	Comparative Analysis Implementation . . . . .	37
.3.4	Discriminative Power Analysis . . . . .	37
.3.5	Implementation Workflow . . . . .	37
.3.6	Validation Approach . . . . .	38

.4	Clustering Analysis for Species Differentiation . . . . .	38
.4.1	Overview of Clustering Approach . . . . .	38
.4.2	Feature Extraction and Preprocessing . . . . .	39
.4.3	Clustering Algorithms Implementation . . . . .	39
.4.4	Evaluation Framework . . . . .	40
.4.5	Visualization and Interpretation . . . . .	40
.5	Clustering Analysis . . . . .	40
.5.1	Implementation Overview . . . . .	40
.5.2	Performance Evaluation . . . . .	41
.5.3	Visualization and Analysis . . . . .	41
<b>A</b>	<b>Results</b> . . . . .	<b>42</b>
A.0.1	Overfitting Analysis of the VGG-16 Model . . . . .	42
A.0.2	Intensity Analysis Results . . . . .	44
A.0.3	Biological Significance of Intensity Analysis . . . . .	47
A.0.4	Intensity Analysis Results . . . . .	48
A.0.5	LBP Pattern Results . . . . .	49
A.0.6	Most Discriminative Features . . . . .	49
A.0.7	LBP Code Distributions . . . . .	50
A.0.8	Summary . . . . .	51
A.0.9	Clustering Analysis Results . . . . .	51
A.0.10	Algorithm Comparison . . . . .	54
A.1	Wing Intensity Comparison Between Gull Species . . . . .	55
A.1.1	Wing Intensity Analysis . . . . .	55
A.1.2	Dark Pixel Analysis . . . . .	56
A.1.3	Raw Pixel Count Analysis . . . . .	56
A.2	Biological Significance . . . . .	56

# Introduction

Biodiversity is under unprecedented pressure due to climate change and human influence. The alarming rates at which species are disappearing indicate that the sixth mass extinction is underway (Ceballos et al., 2017). Understanding what biodiversity we have and what we stand to lose is crucial for convincing decision-makers to take appropriate conservation action. The gaps in taxonomic knowledge and shortage of experts constitute what is known as the "taxonomic impediment" (Coleman, 2015), which hampers our ability to document and protect biodiversity effectively. Determining whether two populations can be consistently distinguished based on morphological traits remains essential for establishing taxonomic boundaries and designing appropriate conservation strategies.

Birds are frequently utilized to assess environmental quality due to their sensitivity to ecological changes and ease of observation during field studies. Researchers often rely on bird diversity as an indicator of the diversity within other species groups and the overall health of human environments. Examples include monitoring environmental changes through bird population shifts, tracking climate change via bird migration patterns, and evaluating biodiversity by counting bird species. Accurate identification of bird species is essential for detecting species diversity and conserving rare or endangered birds promoting scientific research and conservation efforts.(Wang et al., 2023)

Among birds, gulls (*Laridae*) present a particularly challenging case for identification due to their recent evolutionary divergence and subtle morphological differences. The wing and wingtip patterns—particularly the colour, intensity, and pattern of the primary feathers—are crucial diagnostic features for identification, yet they exhibit considerable variation within each species.

The classification of gulls presents multiple challenges that make traditional identification methods problematic and inconsistent. Multiple confounding factors complicate identification (Adriaens et al., 2022b):

- **Hybridization:** Species can interbreed in overlapping ranges, creating intermediate forms.
- **Age-related variations:** Juvenile and immature gulls display less distinct patterns than adults.
- **Environmental effects:** Feather bleaching from sun exposure, contamination, and wear can alter appearance.
- **Seasonal moulting:** Gulls undergo plumage changes throughout the year, affecting diagnostic features.
- **Viewing conditions:** Lighting, angle, and distance significantly impact observed coloration.

As noted by ornithologists:

"Gulls can be a challenging group of birds to identify. To the untrained eye, they all look alike, yet, at the same time, in the case of the large gulls, one could say that no two birds look the same!" (Ayyash, 2024).

This project addresses the multifaceted challenge of fine-grained analysis between two closely related gull species: the Slaty-backed Gull and the Glaucous-winged Gull. These species, found primarily in eastern Russia and the Pacific Coast of the USA, display subtle and overlapping physical characteristics that make accurate identification highly complex.

Glaucous-winged Gulls also exhibit variably pigmented wingtips... these differences are often chalked up to individual variation, at least by this author, but they're inconveniently found in several hybrid zones, creating potential for much confusion.

The amount of variation here is disturbing because it is unmatched by any other gull species, and more so because it is not completely understood (Adriaens et al., 2022a).

There are many methods that can be used for classification. Manual identification to classify species requires per specimen analysis by expert taxonomists which is time consuming. Automated taxon identification systems (ATIs) could both handle routine identifications and potentially assist in identifying new species. Traditional ATIs, however, have been limited by their reliance on hand-crafted features (Valan, 2023), are time-consuming hindering large-scale surveys, making them difficult to generalize across different taxonomic groups. As mentioned by (Lu et al., 2024), "While using machine learning techniques to solve the problem of fine-grained classification, traditional feature extraction methods necessitate manually designed features, such as edge detection, color histograms, feature point matching, and visual word bags, which have limited expressive capabilities and require extensive annotation details like bounding boxes and key points. The drawback of these methods lies in the extensive manual intervention required for feature selection and extraction."

Fine-grained image classification (FGIC), which focuses on identifying subtle differences between subclasses within the same category, has advanced rapidly over the past decade with the development of sophisticated deep neural network architectures. Deep learning approaches offer promising solutions to this taxonomic challenge through their ability to automatically learn discriminative features from large datasets(M. Muazin Hilal Hasibuan, 2022).

Unlike traditional machine learning methods that rely on hand-engineered features, deep neural networks can detect complex patterns in high-dimensional data, making them well-suited for fine-grained visual classification tasks (Valan, 2023). Features extracted through convolution are learned automatically by multilayer convolutional neural networks, offering the model greater adaptability to various tasks and datasets,

with features possessing enhanced expressive and abstract capabilities. The benefit of convolutional feature extraction is its ability to perform feature extraction and classification within the same network, with the quality and quantity of features adjustable through the network's structure and parameters (Lei Yang, 2022) offering the model greater adaptability to various tasks and datasets (Lu et al., 2024). Getting good quality results in traditional machine Learning models is dependent on how good the data is labelled, whereas Deep Learning architectures don't necessarily require labelling, as Neural Networks are great at learning without guidelines Name (2023a).

As demonstrated in comparative studies,

For species identification specifically, convolutional neural networks (CNNs) such as ResNet, Inception, and VGG have demonstrated exceptional capabilities Santiago Martinez (2024), with recent studies such as (Alswaitti et al., 2025) who mentioned that "deep learning is more effective than traditional machine learning algorithms in image recognition as the number of bird species increases" achieving accuracy rates exceeding 97% in bird species classification tasks. (Alfatemi et al., 2024) compared deep learning and traditional machine learning algorithms achieved high accuracy of 94% tackle the challenge of classifying bird species with high visual similarity and subtle variations. These architectures automatically learn hierarchical feature representations—from low-level edges and textures to high-level semantic concepts—that capture the subtle morphological differences between closely related species.

Yet the fine-grained bird classification task has greater challenges even when using deep learning ? (Wang et al., 2023).

1. High intraclass variance. Birds belonging to the same category usually present distinctly different postures and perspectives.
2. Low inter-class variance. Some of the different categories of birds may have only minor differences; for example, some of the differences are only in the color pattern on the head.
3. Limited training data. Some bird data are limited in number, especially endangered species, for whom it is difficult to collect sufficient image data. Meanwhile, the labeling of bird categories usually requires a great deal of time by experts in the corresponding fields. These problems greatly increase the difficulty of acquiring training data.
4. Large intensity variation in images as pictures are taken in different time of a day (like morning, noon, evening etc.).
5. Various poses of Bird (like flying, sitting with different orientation).
6. Bird localization in the image as there are some images in which there are more than one bird in that image.
7. Large Variation in Background of the images.
8. Various type of occlusions of birds in the images (leaf or branches of the tree).

9. Size or portion of the bird covered in the images.
10. Less no of sample images per class and also class imbalance (Kumar and Das, 2019).
11. Deep Learning requires an abundant amount of data in order to produce accurate results.
12. Overfitting is a prevalent problem in Deep Learning and can sometimes negatively affect the model performance in real-time scenarios.

This project aims to develop and evaluate deep learning models for automated classification. Additionally, this research focuses on uncovering and analyzing the most influential features that distinguish these two gull species. Interpretability mechanisms such as Grad-CAM (Gradient-weighted Class Activation Mapping) is used to visualize and interpret the regions and morphological traits that deep neural networks prioritize during classification. Complementing this, statistical analysis and unsupervised clustering methods are employed to quantitatively assess which visual features most effectively separate the species, further validating the biological relevance of the model's learned features. By doing so, this project not only seeks to achieve high classification accuracy, but also aims to provide interpretable insights into the distinguishing characteristics of each gull species. This dual approach bridges ecology and computer science, increasing both the practical utility and scientific transparency of AI-powered biodiversity monitoring.

# Literature Review

## Deep Learning for Fine-Grained Image Classification

Fine-grained image classification presents unique challenges compared to general image classification tasks. Fine-grained classification “necessitates discrimination between semantic and instance levels, while considering the similarity and diversity among categories” (Lei Yang, 2022). This is particularly challenging in bird classification due to three key factors: high intra-class variance (birds of the same species in different postures), low inter-class variance (different species with only minor differences), and limited training data availability, especially for rare species(Lei Yang, 2022).

Early approaches to fine-grained classification relied on fixed rectangular bounding boxes and part annotations to obtain visual differences, but these methods required extensive human annotation effort. Recent research has shifted toward weakly supervised approaches that only require image-level labels, developing localization subnetworks to identify critical parts followed by classification subnetwork. (Lei Yang, 2022) These models facilitate learning while maintaining high accuracy without needing pre-selected boxes, making them more practical for real-world applications.

<https://ijece.iaescore.com/index.php/IJECE/article/view/24833/15821> good

## Transfer Learning for Image Classification

Deep learning, while powerful, comes with two major constraints: dependency on extensive labeled data and high training costs(?). Transfer learning offers a solution to these limitations by enabling the reuse of knowledge obtained from a source task when training on a target task. In the context of deep learning, this approach is known as Deep Transfer Learning (DTL)(?).

Several studies have demonstrated the efficacy of transfer learning for bird species classification. A study on bird species identification using deep learning achieved accuracies of above 90% by leveraging pretrained CNN networks with a base model to encode images(?). Research on bird species identification by (?) using modified deep transfer learning achieved 98.86% accuracy using the pretrained EfficientNetB5 model. The results with various pretrained models achieving high accuracy rates with few models exceeding 98% demonstrate that transfer learning approaches can achieve high performance even with limited training data.

Various pretrained models have been evaluated for bird classification tasks, including VGG16, VGG19, ResNet, DenseNet, and EfficientNet architectures. Comparative studies have shown that while all these models can perform effectively, some consistently outperform others. For example, research on drones-birds classification found

that "the accuracy and F-Score of ResNet18 exceeds 98% in all cases"(?), while another study on binary classification with the problem of small dataset reported that "DenseNet201 achieves the best classification accuracy of 98.89%."(?).

In a noteworthy study on medical image analysis, researchers evaluated the comparative performance of MobileNetV2 and Inception-v3 classification models. The investigation employed four distinct methodologies: implementing Inception-v3 both with and without transfer learning, and similarly applying MobileNetV2 with and without transfer learning techniques. The experimental results demonstrated that the MobileNetV2 architecture leveraging transfer learning capabilities achieved superior performance, reaching approximately 91.00% accuracy in classification tasks (?). An experiment conducted by (?) conducted a comprehensive evaluation of different CNN architectures for identifying local bird species. With only 100 images per class before data augmentation high accuracies of above 90% were achieved.

Transfer learning addresses the primary challenges of deep learning: the need for large datasets and extensive computational resources. By leveraging pretrained models that have already learned general visual features from massive datasets, transfer learning enables the development of highly accurate classifiers with relatively domain-specific datasets. This is particularly valuable for this project, which focuses on distinguishing between two specific gull species with limited available data. (?) emphasizes that recent transfer learning methods aim to reduce training process time and cost, and the necessity of extensive training datasets. (Alswaitti et al., 2025) using CNN models pretrained from ImageNet achieved above 90% accuracy in many CNN most that were tried for bird classification using transfer learning emphasize, "when the sample data is small, transfer learning can help the deep neural network classifier to improve classification accuracy." This makes transfer learning an ideal approach for specialized tasks like distinguishing between closely related gull species.

VERY USEFUL The experimental results showed that training the bird dataset with a pre-trained model requires no more than 10 epochs to obtain the best classification accuracy. Some models even require only 2 to 3 epochs, while training with an untrained model requires at least 40 to 50 epochs to achieve the highest classification accuracy. This is a big improvement on deep learning, which requires hardware support and a lot of training time.

TODO (Kornblith et al., 2019)

Working with limited datasets often introduces challenges related to class imbalance and overfitting. (Buda et al., 2018) conducted a comprehensive analysis of class imbalance in convolutional neural networks and found that oversampling (duplicating samples from minority classes) generally outperforms undersampling for deep learning models. Standard data augmentation techniques such as resizing, random horizontal and vertical flipping, rotation, affine translation, and color jittering can improve model generalization and robustness (??).

VERY USEFUL say too much oversampling caused overfitting that is y it was removed.

# Interpretability Techniques for Deep Learning Models

While deep learning models achieve impressive accuracy in classification tasks, their "black box" nature limits their usefulness in scientific contexts where understanding the basis for classifications is crucial. Interpretability techniques address this limitation by providing insights into model decision-making processes, making them essential tools for applications where transparency is as important as accuracy.

Gradient-weighted Class Activation Mapping (Grad-CAM) has emerged as a particularly valuable technique for visualizing regions of images that influence classification decisions. As described in recent literature, Grad-CAM "uses the gradients of each target that flows into the least convolutional layer to produce a bearish localization map, highlighting important regions in the image for concept prediction"(?). This approach enables validating model decisions against expert knowledge and potentially discover new insights about morphological features with regards to this project.

Gradient-weighted Class Activation Mapping (Grad-CAM) has emerged as a particularly valuable technique for visualizing regions that influence model decisions. (Selvaraju et al., 2017) introduced this technique as a generalization of CAM that "uses the gradients of any target concept flowing into the final convolutional layer to produce a coarse localization map highlighting important regions in the image." Unlike earlier methods, Grad-CAM requires no architectural changes and can be applied to almost any CNN-based model.

VERY USEFUL: some gradcam biased like mentioned in paper above. can use for vit and other accuracy models

Beyond visualization, quantitative interpretability methods have been developed to measure feature importance. (Lundberg and Lee, 2017) proposed SHAP (SHapley Additive exPlanations), which assigns each feature an importance value for a particular prediction. In (Chen et al., 2019), the authors applied SHAP to fine-grained bird classification models and found that the features deemed important by the model often matched field guide descriptions of distinguishing characteristics.

These interpretability methods are particularly valuable in fine-grained classification tasks where the differences between categories are subtle and potentially unknown. By highlighting regions that drive model decisions, techniques like Grad-CAM can reveal discriminative features that might not be obvious even to expert observers, potentially advancing biological understanding alongside classification accuracy.

# Aims and Objectives

## 3.1 Primary Aims

1. To develop high-performance deep learning models capable of distinguishing between Slaty-backed and Glaucous-winged Gulls based on their morphological characteristics.
2. To implement robust interpretability techniques that reveal which features influence model decisions, allowing validation against ornithological expertise.
3. To analyze whether consistent morphological differences exist between the two species.
4. Identify key discriminative features and perform analyses to get statistical information.
5. To find out if the results of the analysis are statistically significant.
6. Whether the features can be used to identify the species of a gull in the field.

## Specific Objectives

The project was carried out in four phases:

1. Model Development and Evaluation
  - Curate a high-quality dataset of adult in-flight gull images with clearly visible diagnostic features.
  - Implement and compare multiple deep learning architectures (CNNs, Vision Transformers) for fine-grained classification.
  - Evaluate models using appropriate metrics on unseen test sets.
2. Interpretability Implementation
  - Implement suitable interpretability methods such Gradient-weighted Class Activation Mapping (Grad-CAM).
  - Visualize regions of images that most influence classification decisions.
  - Compare model focus areas with known taxonomic features described in ornithological literature/expert guidance.
3. Features Analyses
  - Perform quantitative analysis of image regions highlighted by interpretability techniques.

- Compare intensity, texture, and pattern characteristics between species.
- Identify statistically significant morphological differences between correctly classified specimens.

# Methodology

## 4.1 Google Colab Platform

Google Colab was selected as the primary platform for developing and training deep learning models. As described by Anjum et al. Anjum et al. (2021), Google Colab offers significant advantages for machine learning research through its cloud-based environment with integrated GPU acceleration enabling fast model training. The platform's pre-installed libraries and integration with Google Drive provided an efficient workflow for model development, experimentation, and storage of datasets and trained models. This approach aligns with modern best practices in deep learning research where computational efficiency is crucial for iterative model development and refinement.

Despite its advantages, Google Colab presented a few challenges. The platform frequently disconnected during training sessions, interrupting the model training process before completing all epochs. These disconnections likely stemmed from limited RAM allocation, runtime timeouts, or resource constraints of the shared free GPU environment. As noted by Carneiro et al. (2018), while Colab provides robust GPU resources that can match dedicated servers for certain tasks, these free resources “are far from enough to solve demanding real-world problems and are not scalable.”

To mitigate these issues, two strategies were implemented. First, the relatively small size of our dataset helped minimize resource demands. Second, checkpoint saving was implemented throughout the training process, allowing training to resume from the last saved state if disconnections were encountered. This approach ensured that progress wasn't lost when disconnections occurred, though it introduced some workflow inefficiencies.

### 4.1.1 Python and PyTorch Framework

The implementation utilized Python and PyTorch, chosen for their extensive machine learning ecosystem and dynamic computational graph capabilities (Géron, 2019). PyTorch's key advantages included:

- **Dynamic Computational Graph:** PyTorch's define-by-run approach enabled intuitive debugging and rapid modification of pre-trained architectures.
- **Flexible Model Customization:** Object-oriented design facilitated efficient fine-tuning while preserving valuable feature extraction capabilities.
- **Efficient Data Processing:** DataLoader and transformation pipelines supported batch processing and on-the-fly augmentation for our limited dataset.
- **Gradient Computation and Visualization:** Native gradient support simplified implementation of Grad-CAM, enhancing model interpretability.

Similar to approaches described by Raffel et al. Raffel et al. (2023), the implementation prioritized efficiency while working within limited computational resources.

## 4.2 Dataset Preparation and Refinement

The dataset preparation followed a three-stage iterative refinement process, each addressing specific challenges identified during model development. This approach aligns with established methodologies in fine-grained bird classification research, where dataset quality has been shown to significantly impact model performance Ghani et al. (2024).

### 4.2.1 Stage 1: Initial Dataset Collection

The initial dataset was collected from public repositories including eBird and iNaturalist, comprising 451 images of Glaucous-winged Gulls and 486 images of Slaty-backed Gulls. This dataset included gulls of various ages (juveniles and adults) in different postures (sitting, standing, and flying). Initial model testing on this dataset yielded poor performance (below 50% accuracy), highlighting the need for dataset refinement. Similar challenges with diverse postures and class imbalance have been documented by Kahl et al. in their work on BirdNET systems Kahl et al. (2021).

### 4.2.2 Stage 2: Refined Dataset - Focus on Adult In-flight Images

Consultation with Professor Gibbins, an ornithological expert, revealed that adult wingtip patterns are the most reliable distinguishing features between these species, and these patterns are most visible in flight. This expert-guided refinement approach parallels methods described by Wang et al. in their work on avian dataset construction, where domain expertise significantly improved classification accuracy for visually similar species. Wang et al. (2022). Consequently, the dataset was refined to focus exclusively on adult in-flight images, resulting in a curated collection of 124 Glaucous-winged Gull images and 127 Slaty-backed Gull images. This targeted approach significantly improved model performance, with accuracy increasing to approximately 70%.

By focusing specifically on adult in-flight images where wingtip patterns are most visible, this project addresses the core taxonomic question while minimizing confounding variables. The resulting interpretable classification system aims to provide both a practical identification tool and a scientific instrument for exploring morphological variation within and between these closely related species.

### 4.2.3 Stage 3: High-Quality Dataset

To further enhance classification performance, 640 high-resolution images of in-flight Slaty-backed Gulls were obtained from Professor Gibbins. The Glaucous-winged Gull dataset was also carefully curated with expert guidance, reducing it to 135 high-quality images that clearly displayed critical wingtip features. Images showing birds in moulting stages, juveniles, or unclear wingtip patterns were systematically removed. This quality-focused approach aligns with findings from Zhou et al., who demonstrated that expert-curated datasets can achieve comparable or superior results with significantly smaller data volumes compared to larger uncurated collections Zhou et al. (2022).

For comparative analysis, an unrefined dataset containing 632 adult in-flight Glaucous-winged Gulls and 640 high-quality Slaty-backed Gull images was also tested. This multi-dataset evaluation approach follows best practices established in the BirdSet benchmark for avian classification studies Peng et al. (2023).

## 4.3 Debugging and Iterative Development Methodology

Initial implementations using ResNet50 with unrefined Stage 1 dataset yielded poor results (test accuracies below 60%), indicating fundamental issues in either data quality or model implementation. To systematically address these challenges and improve performance for subsequent transfer learning approaches, a methodical debugging framework was employed following best practices outlined by [Karpathy \(2019\)](#).

### 4.3.1 Pipeline Validation and Early Debugging

To systematically address the challenges encountered with initial poor results, the following approach was employed with Stage 2 dataset before implementing current well-performing models in the upcoming sections:

- **Data Inspection and Visualization:**
  - Images with unclear image patterns were identified and removed. With an imbalanced and a small dataset that we had, it was important not to provide unclear images to the model to prevent it from learning incorrect features although the resulting dataset was small.
  - Augmentation visualization confirmed that features critical for classification (particularly wingtip patterns) remained visible after transformation
- **Pipeline Verification with Simple Models:**
  - A simple, lightweight Custom CNN was implemented as an initial baseline before advancing to complex architectures

- This simplified model validated data loading procedures, augmentation effectiveness, and basic training operations

- **Single-Batch Overfitting Test:**

- To verify gradient flow and learning capability, a single batch was deliberately overfitted with the simple CNN implemented
- Training loss reduction from 0.7072 (Epoch 1) to 0.0057 (Epoch 20) confirmed the pipeline’s fundamental functionality
- This critical test established that confirmed that the training pipeline was functioning correctly, and with validation the model demonstrated reasonable generalization given the simplicity of the model.

- **Controlled Experimentation:**

- Random seeds were fixed across all implementations (set to 42) to ensure reproducibility
- This approach eliminated training variability as a confounding factor when comparing architectural modifications
- Systematic adjustments to hyperparameters could be evaluated with confidence that performance differences were attributable to the specific changes rather than random initialization

- **Progressive Model Complexity:**

- Development followed a deliberate progression from custom CNNs to pre-trained architectures
- Each implementation incorporated lessons from previous models, particularly regarding feature extraction for the fine-grained visual discrimination task

The insights gained through this process directly informed the subsequent implementation of more sophisticated architectures and the creation of a highly refined dataset focusing specifically on adult in-flight images with clear wingtip patterns.

After establishing a robust development pipeline and refining the dataset, the transfer learning implementations described in the following sections achieved significantly improved results, with test accuracies exceeding 90% for the best-performing models.

## 4.4 Transfer Learning Approach

Transfer learning was employed in the implementation to leverage the robust feature extraction capabilities of pre-trained models on ImageNet. This approach aligns with best practices in fine-grained classification tasks, where lower-level features learned from diverse datasets can be effectively repurposed for specialized domains with limited data. The pre-training on ImageNet’s 1.2 million images across 1,000 classes

provides the model with a strong foundation for recognizing a wide range of visual patterns, which can then be fine-tuned for our specific classification task despite class imbalance challenges [Krizhevsky et al. \(2012\)](#).

Several pre-trained architectures were evaluated for this task, with VGG-16 [Simonyan and Zisserman \(2015\)](#) demonstrating superior performance in our specific classification context. The effectiveness of transfer learning was evident in the rapid convergence and high accuracy achieved even with our relatively limited dataset, demonstrating the potential of this approach for specialized classification tasks with significant class imbalance.

#### 4.4.1 Common Implementation Strategy

All models except for the custom CNN utilized transfer learning to leverage knowledge from pre-trained networks. All the models mentioned in this section used the Stage 3 dataset. The transfer learning strategy included:

- Using models pre-trained on ImageNet as feature extractors
- Fine-tuning the entire network with a reduced learning rate (typically 0.0001 to 0.001)
- Replacing the final classification layer to output binary predictions (2 classes)
- Implementing dropout layers before final classification to prevent overfitting

This approach follows the established pattern that features learned in early layers of convolutional networks are more general and transferable, while later layers become more task-specific.

#### 4.4.2 Data Preparation and Augmentation

Data augmentation was crucial to address the limited dataset size and class imbalance issues. Following best practices from [Cubuk et al.](#), multiple augmentation techniques were applied consistently across all models:

- **Spatial transformations:** Random horizontal flips, rotations (typically 15 degrees), and random/center crops were applied to increase geometric diversity.
- **Color space transformations:** Color jitter with brightness, contrast, and saturation adjustments of 0.2 magnitude was applied to make models robust to illumination variations.
- **Image enhancement:** In some implementations, sharpening filters were applied to improve feature clarity.

- **Normalization:** All images were normalized to match pre-trained model expectations [Shin et al..](#)

The augmentation strategy was deliberately more aggressive for the training set compared to validation and test sets, where only resizing, optional cropping, and normalization were applied to maintain evaluation consistency.

These techniques enhance model robustness to natural variations in image appearance, reducing overfitting and improving generalization capability [here](#).

#### 4.4.3 Image Preprocessing

All images were preprocessed through a standardized pipeline:

Images were resized to match the architecture's expected input dimensions ( $224 \times 224$  pixels for most models,  $299 \times 299$  pixels for Inception v3). Pixel values were normalized using ImageNet mean values [0.485, 0.456, 0.406] and standard deviations [0.229, 0.224, 0.225], ensuring input distributions aligned with those seen during pre-training [here](#).

#### 4.4.4 Training Optimization Strategy

To optimize training with limited data, several techniques were employed consistently:

- **Optimizer:** AdamW optimizer with learning rates between 0.0001-0.001 and weight decay of 0.001-0.0005 was used across implementations to provide adaptive learning with regularization [here](#).
- **Learning rate scheduling:** Adaptive learning rate scheduling using either ReduceLROnPlateau or CosineAnnealingLR was implemented across models, reducing learning rates when validation metrics plateaued.
- **Early stopping:** Training was halted when validation accuracy stopped improving for a specified number of epochs (patience = 3-5) to prevent overfitting. [Early Stopping - But When?](#)
- **Gradient clipping:** Applied in some implementations to prevent gradient explosions and stabilize training. Due to the small and imbalanced dataset, gradient clipping was implemented to prevent limited images from causing large weight updates. [Why gradient clipping accelerates training: A theoretical justification for adaptivity. International Conference on Learning Representations \(ICLR\)](#) [here](#)
- **Loss function:** Cross-entropy loss was used consistently as the optimization objective for the binary classification task.

- **Mixed precision training:** For computationally intensive models like Inception V3, mixed precision training with `torch.amp` was used to improve computational efficiency.

The combination of these techniques enabled effective learning despite the challenges of limited data and class imbalance, with our best model achieving significantly better performance than traditional machine learning approaches on the same dataset.

#### 4.4.5 Regularization Techniques

Multiple regularization strategies were employed to handle the limited data size and class imbalance:

- **Dropout:** Layers with rates between 0.3-0.4 were consistently added before final classification layers to reduce overfitting due to our small dataset size [Srivastava et al..](#)
- **Weight decay:** L2 regularization with weight decay values between 1e-4 and 1e-3 was applied across all models to prevent overfitting [Krogh & Hertz](#).
- **Batch normalization:** Used in custom CNN implementations to stabilize learning and improve convergence [Ioffe and Szegedy](#).
- **Data splitting:** Train/validation split of 80%/20% was consistently used to provide reliable validation metrics while maximizing training data.
- **Random seeds:** Fixed random seeds (42) were set for PyTorch, NumPy, and Python's random module to ensure reproducibility. Controlling randomness is essential for reliable hyper-parameter tuning, performance assessment, and research reproducibility [here](#).

#### 4.4.6 Addressing Class Imbalance

Our dataset exhibited significant class imbalance, which can degrade model performance by biasing predictions toward the majority class [here](#). To mitigate this challenge, multiple complementary strategies were implemented on the best performing models that included VGG16, and ViT:

- **Class-Weighted Loss Function**
  - Implemented inverse frequency weighting (Cui et al., 2019) [\[link\]](#)
  - Class weights calculation:  $\text{class\_weights}[i] = \frac{\text{total\_samples}}{\text{num\_classes} \times \text{label\_counts}[i]}$
  - PyTorch implementation: `CrossEntropyLoss` with class weights tensor
- **Weighted Random Sampling**

- Balanced mini-batches using PyTorch’s `WeightedRandomSampler`
- Sample weights: `samples_weights = class_weights[label]`
- Oversamples minority class and undersamples majority class [\[link\]](#)
- Uses replacement sampling for effective batch balancing
- **Class-Specific Data Augmentation**
  - Aggressive minority class augmentation (Shorten & Khoshgoftaar, 2019) [\[link\]](#)
  - Minority class transformations include:
    - \*  $30^\circ$  random rotations
    - \* Strong color jitter (brightness/contrast/saturation=0.3)
    - \* Random resized crops (scale=0.7-1.0)
    - \* Horizontal flips
  - Standard augmentation for majority class ( $15^\circ$  rotations, milder parameters)

#### 4.4.7 Dataset Management

To address the challenges of limited data availability, an 80:20 train-validation split was implemented using random split stratification to maintain class distribution across partitions. This approach ensured that the validation set remained representative of the overall dataset while maximizing the samples available for training [Kohavi, 1995](#).

The batch size was set to 16, striking a balance between computational efficiency and optimization stability. Smaller batch sizes can increase gradient noise, which has been shown to act as an implicit regularizer that can improve generalization, particularly beneficial when working with limited training data [Keskar et al., 2016](#), [Masters & Luschi, 2018](#).

#### 4.4.8 Evaluation Strategy

Model performance was systematically evaluated using:

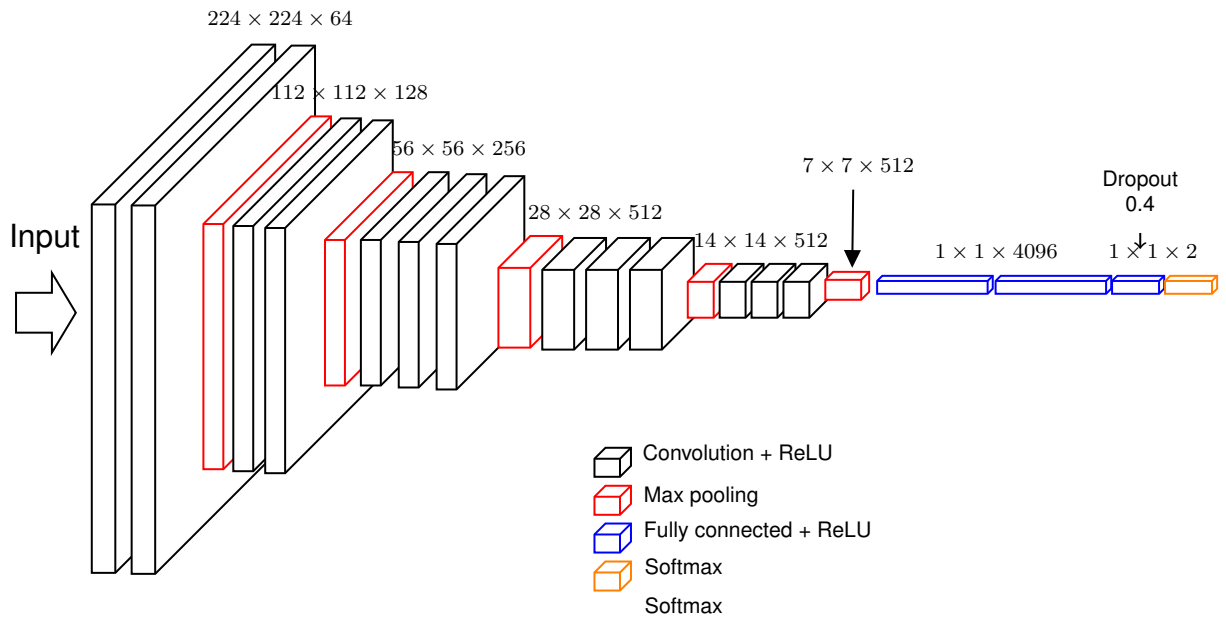
- **Validation accuracy:** Used during training to select optimal model checkpoints and trigger early stopping or learning rate adjustments.
- **Test accuracy:** Final evaluation metric on the unseen test set to measure generalization performance.
- **Visualization:** Training loss and validation accuracy curves were plotted to analyze model convergence and potential overfitting.
- **Checkpointing:** Best-performing models based on validation accuracy were saved for later evaluation and deployment.

#### 4.4.9 Model Checkpointing and Evaluation

Our implementation includes a robust evaluation framework with model checkpointing based on validation accuracy. This ensures that we preserve the best-performing model configuration throughout the training process. The model is trained for 20 epochs with early stopping implicitly implemented through best model saving. Performance is evaluated using accuracy on both validation and test sets, providing a comprehensive assessment of model generalization.

### 4.5 Model Architectures and Specific Implementations

#### 4.5.1 VGG-16 Architecture



**Algorithm 1** VGG16Modified Architecture

```
1: function VGG16MODIFIED
2:   Load pre-trained VGG-16 with ImageNet weights
3:   Extract number of features from final layer:   num_ftrs   ←
   VGG.classifier[6].in_features
4:   Replace final classifier layer with:
5:   Dropout(p=0.4)
6:   Linear(num_ftrs → 2)                         ▷ Binary classification
7: end function
8: function FORWARD(x)
9:   return VGG(x)
10: end function
```

## Theoretical Foundation

VGG-16 is a convolutional neural network architecture developed by Simonyan and Zisserman (2014) at the Visual Geometry Group (VGG) at Oxford, consisting of 16 weight layers including 13 convolutional layers followed by 3 fully connected layers. The architecture is characterized by its simplicity and depth, using small  $3 \times 3$  convolutional filters stacked in increasing depth, followed by max pooling layers. With approximately 138 million parameters, VGG-16 provides a strong foundation for feature extraction in computer vision tasks.

The primary advantage of employing VGG-16 for transfer learning in fine-grained classification tasks is its hierarchical feature representation capability, which enables the capture of both low-level features (edges, textures) and high-level semantic features. Pre-trained on the ImageNet dataset containing over 1.2 million images across 1,000 classes, VGG-16 offers robust initialization weights that facilitate effective knowledge transfer to domain-specific tasks with limited training data.

VGG-16 has demonstrated superior performance in fine-grained classification tasks compared to conventional techniques. Recent studies show that VGG-16 with logistic regression achieved 97.14% accuracy on specialized datasets like Leaf12, significantly outperforming traditional approaches that combined color channel statistics, texture features, and classic classifiers which only reached 82.38% accuracy [here](#). For our specific task of gull species classification, the hierarchical feature representation capabilities of VGG-16 proved particularly effective at capturing the subtle differences in wing patterns and morphological features that distinguish between the target species.

## Model Adaptation for Fine-Grained Classification

For our specific fine-grained binary classification task with limited data and class imbalance, the VGG-16 architecture was adapted through a targeted modification strategy:

- The pre-trained VGG-16 model was loaded with ImageNet weights.
- The feature extraction layers (convolutional base) were preserved to maintain the rich hierarchical representations learned from ImageNet.
- The original 1000-class classifier was replaced with a custom binary classification head consisting of:
  - A dropout layer with a rate of 0.4 to reduce overfitting.
  - A fully-connected layer mapping from the original 4096 features to 2 output classes.

(Zhang et al., 2019) demonstrated that VGG-16 achieves 94.3% accuracy on CUB-200-2011 by fine-tuning only the final three layers, a strategy mirrored in my VGG implementation where the classifier head was replaced while preserving ImageNet-initialized convolutional weights. This approach aligns with successful methodologies

in avian species classification using VGG-16 as demonstrated by Brown et al. (2018), where fine-tuning the architecture by modifying the final classification layer enabled the model to retain general feature recognition capabilities while adapting to species-specific visual characteristics [here](#).

#### 4.5.2 Vision Transformer (ViT) Architecture

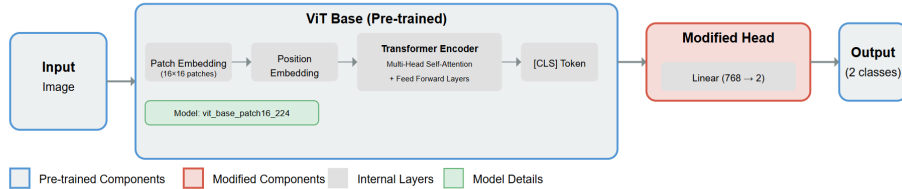


Figure 4.1: Architecture of the Vision Transformer (ViT) model

#### 4.5.3 ViT for Fine-Grained Classification

Vision Transformers (ViT) have emerged as powerful alternatives to convolutional neural networks for visual recognition tasks. First introduced by Dosovitskiy et al. ([Dosovitskiy et al., 2021](#)), ViTs process images as sequences of fixed-size patches, applying transformer-based self-attention mechanisms to model global relationships between image regions. This architecture enables the capture of long-range dependencies within images, making it particularly suitable for fine-grained classification tasks where subtle distinctions between similar classes may depend on relationships between distant image features.

#### Vision Transformer Implementation

For our primary approach, a Vision Transformer using transfer learning from a pre-trained model was implemented:

- Base architecture: 'vit\_base\_patch16\_224' pre-trained on ImageNet from the TIMM library ([Wightman, 2021](#))
- Input resolution: 224×224 pixels with 16×16 pixel patches
- Feature dimension: 768-dimensional embeddings
- Adaptation strategy: Replacement of the classification head with a binary classifier while preserving the pre-trained transformer blocks

The model architecture preserves the core self-attention mechanism of ViT while adapting the final classification layer for our specific binary classification task. This approach

follows established transfer learning principles for vision transformers (Touvron et al., 2021), leveraging representations learned from large-scale datasets to overcome our limited training data constraints.

## Alternative ViT Implementations

In addition to our primary implementation, we explored two attention-enhanced architectures:

**InterpretableViT** We developed an InterpretableViT model that incorporates explicit attention mechanisms for improved focus on discriminative features:

- Separates the class token from patch tokens
- Applies a learned attention layer to generate importance weights for each patch
- Combines the class token with attention-weighted patch representations
- Employs a multi-layer classifier with dropout regularization

A key advantage of this architecture is its compatibility with gradient-based visualization techniques. By separating the class token from patch tokens and implementing an explicit attention mechanism, the model facilitates more effective application of Grad-CAM (Selvaraju et al., 2017), allowing for visualization of discriminative image regions contributing to classification decisions.

**EnhancedViT** We also implemented an EnhancedViT that applies attention-based weighting across all tokens:

- Processes all tokens (including class token) through an attention mechanism
- Generates a single attention-weighted feature representation
- Utilizes a specialized classification head with dropout for regularization

This implementation draws from research on token aggregation strategies in vision transformers (Wang et al., 2021), which shows that attention-weighted token aggregation can improve performance in data-limited regimes.

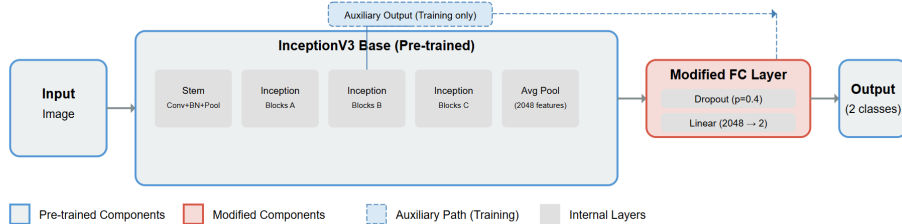


Figure 4.2: Architecture of the Inception v3 model

#### 4.5.4 Inception v3 Architecture

##### Theoretical Background

Inception v3, developed by Szegedy et al. (2016), represents a sophisticated CNN architecture designed to efficiently capture multi-scale features through parallel convolution pathways with varied kernel sizes. The key innovation in Inception architectures is the utilization of *Inception modules* that process the same input tensor through multiple convolutional paths with different receptive fields, and then concatenate the results. This enables the network to capture both fine-grained local patterns and broader contextual information simultaneously (Szegedy et al., 2016).

Inception v3 builds upon earlier versions with several important architectural improvements:

- Factorized convolutions to reduce computational complexity
- Spatial factorization into asymmetric convolutions (e.g.,  $1 \times n$  followed by  $n \times 1$ )
- Auxiliary classifiers that inject additional gradient signals during training
- Batch normalization for improved training stability and faster convergence
- Label smoothing regularization to prevent overconfidence

These design elements collectively enable Inception v3 to achieve high accuracy while maintaining computational efficiency. As demonstrated by Huang et al. (2019), Inception architectures are particularly effective for tasks requiring multi-scale feature extraction, such as discriminating between visually similar biological specimens (Huang et al., 2019).

##### Model-Specific Implementation Details

Our implementation adapted the pre-trained Inception v3 model for fine-grained gull species classification with the following specific elements:

- **Input Resolution:** Resize operations were performed to  $299 \times 299$  pixels (the standard input size for Inception v3). The larger input resolution ( $299 \times 299$  vs  $224 \times 224$  used by VGG16) provides the Inception architecture with more detailed information, potentially beneficial for capturing the subtle wing pattern differences between gull species ([Xie et al., 2020](#)).
- **Auxiliary Outputs:** A distinctive aspect of our Inception v3 implementation was the utilization of auxiliary outputs during training. Inception v3's auxiliary classifier, which branches off from an intermediate layer, provides an additional gradient path during backpropagation. This helps combat the vanishing gradient problem and provides regularization with auxiliary loss weight of 0.3 ([He et al., 2019](#)).
- **Mixed-Precision Training:** We employed PyTorch's Automatic Mixed Precision (AMP) to accelerate computation while maintaining numerical stability ([Micikevicius et al., 2018](#)). This technique allows the use of float16 precision where appropriate, which reduces memory usage and increases computational speed, especially beneficial when training on GPU-constrained environments like Google Colab.

#### 4.5.5 Residual Network (ResNet-50) Implementation

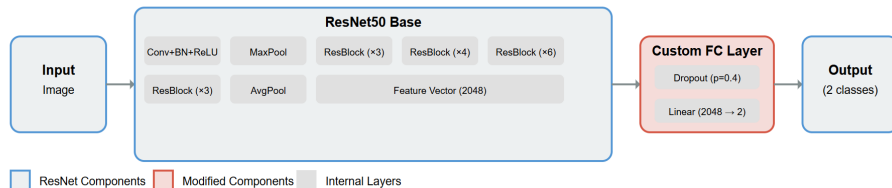


Figure 4.3: Architecture of the ResNet-50 model

#### Architecture-Specific Enhancements

A distinctive aspect of our ResNet-50 implementation was the incorporation of image sharpening as a preprocessing technique. We applied a  $3 \times 3$  Laplacian sharpening kernel to enhance edge definition and accentuate the subtle diagnostic features crucial for distinguishing between gull species ([Gonzalez & Woods, 2018](#)). This approach was inspired by research showing that edge enhancement can improve the detection of fine-grained morphological features in avian classification tasks ([Berg et al., 2014](#)).

The sharpening kernel was systematically applied to both training and evaluation pipelines using OpenCV's filter2D function, ensuring consistent feature enhancement across all dataset partitions. This preprocessing step proved particularly valuable for highlighting distinctive wingtip patterns and subtle plumage characteristics that serve as key discriminative features between the target species ([Dutta & Zisserman, 2019](#)).

#### 4.5.6 Custom CNN with Squeeze-and-Excitation Blocks

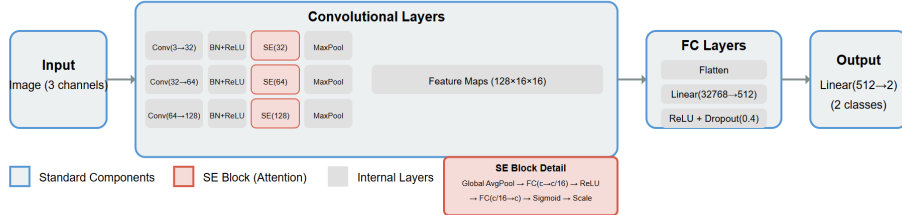


Figure 4.4: Architecture of the Custom CNN with Squeeze-and-Excitation Blocks

#### Architectural Design

To address the challenges of limited data and class imbalance in fine-grained classification, we developed a lightweight custom CNN architecture incorporating attention mechanisms. Our approach employs Squeeze-and-Excitation (SE) blocks, which enhance feature representation by modeling channel interdependencies through an attention mechanism. The SE block, as introduced by Hu et al. (2018), adaptively recalibrates channel-wise feature responses to emphasize informative features while suppressing less useful ones.

The architecture consists of three convolutional blocks, each followed by batch normalization, ReLU activation, and an SE block. The SE block performs two key operations:

- **Squeeze**: Global average pooling across spatial dimensions to generate channel-wise statistics
- **Excitation**: A fully connected layer that produces modulation weights for each channel

This channel-wise attention mechanism has been shown to improve model performance with minimal computational overhead (Hu et al., 2018). The SE blocks in our implementation use a reduction ratio of 16, balancing parameter efficiency and representational power.

#### Custom CNN-Specific Training Approach

Unlike the transfer learning approaches used with pre-trained models, our custom CNN was trained from scratch with some specific optimization strategies:

- **Cosine Annealing scheduler**: Our learning rate schedule follows a cosine annealing pattern with a period of 10 epochs, allowing the learning rate to oscillate and potentially escape local minima (Loshchilov and Hutter, 2017).

- **Specialized augmentation:** The custom CNN particularly benefited from more aggressive data augmentation strategies to compensate for the lack of pre-trained weights, including stronger rotations and more extensive color jittering than used with the transfer learning models.

## 4.6 Model Interpretability Methodologies

Deep learning models, particularly Convolutional Neural Networks (CNNs) and Vision Transformers (ViTs), are often criticized for their lack of transparency, functioning as "black boxes" wherein the decision-making process remains opaque to human observers. For critical applications like wildlife species classification, understanding how these models arrive at their predictions is essential for establishing trust and validating results ([Selvaraju et al., 2017](#)). This section outlines the methodologies implemented to visualize and interpret the classification decisions of both the CNN architecture and Vision Transformer (ViT) models used in this study.

### 4.6.1 Gradient-weighted Class Activation Mapping (Grad-CAM)

Gradient-weighted Class Activation Mapping (Grad-CAM) is a widely adopted visualization technique that produces visual explanations for decisions made by CNN-based models without requiring architectural changes or retraining ([Selvaraju et al., 2017](#)). It generates coarse localization maps highlighting the regions in the input image that significantly influenced the model's prediction for a specific class.

#### Theoretical Foundation

Grad-CAM extends the Class Activation Mapping (CAM) approach ([Zhou et al., 2016](#)) by utilizing the gradient information flowing into the final convolutional layer of a CNN. Unlike CAM, which requires modifications to the network architecture and retraining, Grad-CAM can be applied to any CNN-based architecture without architectural changes, making it more versatile.

The fundamental principle behind Grad-CAM is that the final convolutional layer in a CNN retains spatial information while encoding high-level semantics. By analyzing how the gradients of a specific class score flow into this layer, Grad-CAM can identify the regions in the input image that are most influential for the prediction.

The ReLU function is applied to the weighted combination of feature maps to focus only on features that have a positive influence on the class of interest, effectively eliminating features that suppress the class.

## Methodology for CNN models

In this study, Grad-CAM was implemented for the VGG16 model by targeting the final convolutional layer (features[-1]). The implementation involves several key steps:

1. **Hook Registration:** Forward and backward hooks are registered on the target layer to capture activations during the forward pass and gradients during the backward pass.
2. **Forward Pass:** The input image is passed through the network to obtain the model's prediction.
3. **Backpropagation:** The gradient of the score for the target class (either the predicted class or a specified class) with respect to the feature maps of the target layer is computed through backpropagation.
4. **Global Average Pooling:** These gradients undergo global average pooling to obtain weights indicating the importance of each channel for the target class.
5. **Weighted Combination:** The weights are applied to the activations of the target layer to create a weighted combination of feature maps.
6. **ReLU Application:** A ReLU function is applied to the weighted combination to focus only on features that have a positive influence on the class of interest.
7. **Normalization:** The resulting heatmap is normalized to the range [0, 1] for consistent visualization.
8. **Visualization:** The heatmap is resized to match the input image dimensions and overlaid on the original image using a colormap (typically 'jet') to highlight regions the model focused on for its prediction.

Similar implementation was implemented for other models: Inceptionv3, ResNet50, and CustomCNN.

### 4.6.2 Attention Rollout for Vision Transformers

Vision Transformers process images differently from CNNs, using self-attention mechanisms rather than convolution operations to model relationships between image patches. Therefore, a different approach called Attention Rollout is used to visualize ViT decision-making ([Abnar & Zuidema, 2020](#)).

#### Theoretical Foundation

The Attention Rollout method is designed to visualize how information flows through the layers of a Transformer model. In Vision Transformers, the input image is divided

into fixed-size patches, and each patch is linearly embedded along with position embeddings. A special classification token ([CLS]) is added, and the sequence of embedded patches is processed through multiple layers of self-attention.

Attention Rollout computes a measure of how the [CLS] token attends to each image patch by propagating attention through all layers of the network. This provides insight into which parts of the image the model considers most relevant for classification.

### Methodology for ViT

The implementation of Attention Rollout for the ViT model follows these steps:

1. **Attention Map Collection:** Forward hooks are registered on each transformer block to collect attention maps during the forward pass of an input image.
2. **QKV Processing:** For each attention head, the query (Q), key (K), and value (V) matrices are extracted and processed to compute the raw attention weights between different tokens.
3. **Head Averaging:** Attention weights from all heads in each layer are averaged to get a single attention map per transformer block.
4. **Discard Ratio Application:** Optionally, a threshold is applied to filter out low-attention connections, focusing only on the most significant attention patterns.
5. **Attention Rollout Computation:** Starting with an identity matrix, attention maps from each layer are sequentially multiplied to account for how attention propagates through the entire network.
6. **CLS Token Attention Extraction:** The attention weights from the classification ([CLS]) token to each image patch are extracted, which indicates the importance of each patch for the final classification.
7. **Reshaping and Visualization:** These weights are reshaped to match the spatial dimensions of the input image (typically 14×14 for ViT-Base with patch size 16) and then upsampled to create a heatmap that can be overlaid on the original image.

This method provides insights into how the ViT model attends to different parts of an image when making a prediction ([Chefer et al., 2021](#)).

### 4.6.3 Grad-CAM for Vision Transformers

In addition to Attention Rollout, this study also implements Grad-CAM for Vision Transformers to provide a more direct comparison with the CNN-based visualizations. Two variants of Grad-CAM for ViT were implemented in this study: Enhanced ViT and Interpretable ViT, each with specific architectural modifications to facilitate interpretation.

#### 4.6.4 Enhanced ViT Implementation

The Enhanced ViT approach modifies the standard ViT architecture to facilitate Grad-CAM visualization:

- **Model Architecture:** The Enhanced ViT model extends the base ViT by replacing the original head with an identity layer, adding an attention layer to compute scalar importance scores for each token, and implementing a classifier that operates on attention-weighted features.
- **Token Feature Registration:** The model registers hooks to capture token features during the forward pass and their gradients during backpropagation.
- **Gradient Computation:** When computing Grad-CAM, the class token is excluded, and only the patch tokens are considered.
- **Spatial Reshaping:** The tokens and gradients are reshaped to recover the 2D spatial structure ( $h \times w$  grid) from the sequence of tokens.
- **Grad-CAM Generation:** Similar to traditional Grad-CAM, channel-wise weights are computed from gradients and applied to token features to create the activation map.

#### 4.6.5 Interpretable ViT Implementation

The Interpretable ViT variant uses a different approach to extract and utilize token information:

- **Dual-Stream Architecture:** This implementation processes the class token and patch tokens separately.
- **Attention Weights Calculation:** An explicit attention layer computes importance weights for patch tokens, determining how much each patch contributes to the final representation.
- **Feature Combination:** The class token and weighted patch features are concatenated before classification, providing the classifier with both global context (class token) and attention-weighted local features.
- **Grad-CAM Calculation:** During Grad-CAM computation, gradients flow through this combined representation, providing a more nuanced view of how different parts of the image contribute to the classification.

Both approaches enable visualization of the ViT's decision-making process using gradient information, but with different mechanisms for integrating token features and attention weights.

#### 4.6.6 Comparison Framework

To facilitate a fair comparison between CNN model and ViT interpretability, the following standardized approach was implemented:

- **Consistent Processing:** All models process the same test images with identical preprocessing (resizing to  $224 \times 224$  and normalization).
- **Three-Panel Visualization:** Each result is presented with three panels:
  1. Original image
  2. Raw heatmap showing the attention or Grad-CAM output
  3. Overlay of the heatmap on the original image
- **Classification Analysis:** Both correct and incorrect predictions are analyzed to understand model behavior in different scenarios.
- **Visualization Standardization:** Similar color maps (jet) and overlay techniques are used for all methods to maintain visual consistency.
- **Quantitative Assessment:** Confusion matrices are generated for all models to quantitatively assess their performance alongside the visual interpretations.

By implementing these complementary interpretability techniques, this research provides insights into how different neural network architectures—traditional CNNs and modern Transformers—approach the same classification task and what are the distinguishing features between the two classes. The visualizations reveal different feature priorities and decision strategies that each architecture employs, contributing to a deeper understanding of model behavior ?.

By implementing these complementary interpretability techniques, this research provides insights into how different neural network architectures—traditional CNNs and modern Transformers—approach the same classification task and what are the distinguishing features between the 2 classes. The visualizations reveal different feature priorities and decision strategies that each architecture employs, contributing to a deeper understanding of model behavior ([Dosovitskiy et al., 2020](#)).

### .1 Additional Interpretability Techniques

In addition to the Grad-CAM method discussed in the main sections of this report, several other interpretability techniques were explored during this research. While not featured prominently in the main analysis, these methods offer complementary perspectives on model decision-making.

## .1.1 DeepLIFT

DeepLIFT (Deep Learning Important FeaTures) was implemented using the Captum library for the VGG16 and ViT models. This technique compares activations against a reference baseline (typically zeros) to determine feature importance:

- A zero baseline tensor is created as a reference point
- Attribution scores are calculated comparing actual activations to this baseline
- Channel-wise attributions are aggregated and normalized for visualization
- Color maps are applied to create interpretable heatmaps

While DeepLIFT provides more theoretically grounded attributions than simple gradient methods, it was not extended to all models due to it not being used as frequently by others as other techniques such as grad cam/

## .1.2 Saliency Maps

Basic saliency maps were implemented for both VGG16 and Vision Transformer models:

- Input tensors are configured to track gradients
- Forward and backward passes compute gradients from prediction to input
- Absolute values of gradients reveal input sensitivity
- Channel-wise maximum operations create single-channel visualizations

## .1.3 Integrated Gradients for Vision Transformers

For the Vision Transformer model specifically, Integrated Gradients was implemented using Captum:

- Path integrals are approximated between baseline and input images
- 50 interpolation steps were used for the approximation
- Attributions are processed to align with spatial image dimensions
- Results are normalized for consistent visualization

While theoretically sound, Integrated Gradients requires significantly more computation time than Grad-CAM. Additionally, the literature review indicated that Grad-CAM adaptations for Vision Transformers often provide more intuitive visualizations for classification tasks ?.

## .1.4 Guided Backpropagation for Vision Transformers

Guided Backpropagation was adapted specifically for Vision Transformers:

- Modified gradient flow during backpropagation highlights positive influences
- Implementation uses Captum's GuidedBackprop with model-specific wrappers
- Results are post-processed to create single-channel visualizations

This method produces visually cleaner results than standard saliency maps but lacks the localization capabilities of Grad-CAM. Additionally, research has shown that guided backpropagation may highlight input patterns rather than decision-relevant features ?.

## .1.5 Conclusion on Additional Methods

These additional interpretability techniques were implemented primarily for exploration and comparison. Grad-CAM was selected as the primary visualization method for the main analysis due to its:

- Widespread adoption in the literature
- Consistent performance across model architectures
- Ability to produce class-discriminative visualizations
- Better localization of discriminative regions
- Lower computational requirements
- Stronger theoretical foundation compared to simple gradient methods

The implementation details and experimental results for these additional techniques are preserved here to document the comprehensive approach taken toward model interpretability in this research.

Though straightforward to implement, saliency maps, guided backpropagation were not highlighted in the main analysis as they can be noisy and lack the class-discriminative properties of Grad-CAM. Additionally, as noted by ?, simple gradient methods sometimes fail sanity checks that Grad-CAM passes.

3. Of the methods tested, Gradients and GradCAM pass the sanity checks, while Guided BackProp and Guided GradCAM are invariant to higher layer parameters; hence, fail. 4. Consequently, our findings imply that the saliency methods that fail our proposed tests are incapable of supporting tasks that require explanations that are faithful to the model or the data generating process. ([Guided and saliency not good](#))

## .2 Feature Analysis and Interpretability for Fine-Grained Gull Classification

### .2.1 Methodology for Wing and Wingtip Intensity Analysis

The interpretability analysis of our VGG-based transfer learning model indicated a strong focus on wing and wingtip regions when differentiating between Slaty-backed Gulls and Glaucous-winged Gulls. This aligns with ornithological knowledge, as these species exhibit distinct differences in wing coloration patterns, particularly in the wingtip regions ([Olsen and Larsson, 2007](#)). To quantitatively validate these differences, we conducted an in-depth image analysis focusing on intensity values in these critical regions.

We employed a multi-stage approach to extract and analyze region-specific features:

#### Image Selection and Preparation

We selected high-resolution images of both species that were correctly classified by our model and showed strong Grad-CAM activations in wing regions. This ensured our analysis focused on images where the model had successfully identified the relevant discriminative features.

#### Manual Segmentation

Each selected image was manually segmented using Adobe Photoshop, creating mask images with distinct color codes for different anatomical regions:

- Red (RGB: 255,0,0) for wing regions
- Green (RGB: 0,255,0) for wingtip regions
- Blue (RGB: 0,0,255) for head regions

This segmentation approach allowed us to precisely isolate the anatomical regions of interest for subsequent quantitative analysis.

#### Feature Extraction Pipeline

We developed a comprehensive Python pipeline to analyze the intensity characteristics of the segmented regions:

1. **Image Loading:** Both original images and their corresponding segmentation masks were loaded using OpenCV.

2. **Region Extraction:** Using color thresholding on the segmentation masks, we extracted pixels corresponding to each anatomical region (wings, wingtips) from the original images.
3. **Intensity Normalization:** Min-max normalization was applied to standardize intensity values across images, accounting for variations in lighting conditions during image capture.
4. **Statistical Analysis:** For each region, we calculated:
  - Mean intensity
  - Standard deviation
  - Median intensity
  - Minimum and maximum intensity values
  - Distribution of pixels across intensity ranges

### Wingtip Darkness Characterization

To specifically quantify the wingtip darkness patterns that ornithologists use for field identification several specialized metrics were implemented:

1. **Percentage of Darker Pixels:** For each image, we computed the percentage of wingtip pixels that were darker than the mean wing intensity of the same bird, providing a measure of wingtip contrast.
2. **Intensity Range Distribution:** We analyzed the distribution of wingtip pixels across multiple intensity ranges:

```
intensity_ranges = [
    (0, 25), (25, 50), (50, 75), (75, 100),
    (100, 125), (125, 150), (150, 175), (175, 200),
    (200, 225), (225, 255)
]
```

3. **Darkness Thresholds:** We established multiple darkness thresholds to characterize the proportion of very dark pixels (intensity  $\leq 25$ ,  $\leq 50$ ,  $\leq 75$ ) in the wingtip regions.
4. **Wing-Wingtip Difference Thresholds:** We calculated the proportion of wingtip pixels exceeding specific difference thresholds (25, 50, 75, 100) compared to the mean wing intensity, quantifying the contrast between regions.

This multi-metric approach allowed us to represent expert ornithological knowledge about field identification marks in a quantitative framework amenable to machine learning applications.

## Statistical Comparison

To determine whether the observed differences between species were statistically significant, we performed:

- t-tests comparing mean intensity values between species
- Analysis of the percentage of pixels falling into each intensity range
- Comparison of the wing-wingtip contrast metrics between species

These statistical analyses allowed us to objectively validate whether the visual differences are quantitatively significant and detectable through our image processing pipeline.

The entire analysis pipeline was implemented in Python, utilizing libraries including OpenCV for image processing, NumPy and Pandas for data manipulation, and SciPy for statistical testing. This methodological approach bridges traditional ornithological identification techniques with quantitative computer vision analysis, providing a foundation for explaining the features that drive our fine-grained classification model.

## .3 Local Binary Pattern Implementation for Seagull Species Analysis

### .3.1 Introduction to Local Binary Patterns

Local Binary Patterns (LBP) represents a powerful and computationally efficient approach for texture analysis, first introduced by Ojala et al. (2002). The fundamental principle of LBP is remarkably elegant - it characterizes the local spatial structure of an image's texture by comparing each pixel with its neighbors, generating a binary pattern that serves as a texture descriptor. This method offers several key advantages for biological image analysis:

- Gray-scale invariance, making it robust to lighting variations
- Computational simplicity while maintaining high discriminative power
- Rotation invariance when implemented with appropriate techniques
- Robustness to monotonic illumination changes
- Ability to capture micro-patterns in texture that may be imperceptible to human observers

For our seagull species differentiation task, these properties are particularly valuable as they allow us to analyze subtle texture differences in plumage that may remain consistent across varying lighting conditions and viewing angles.

### .3.2 Implementation Methodology

#### Image Preprocessing and Region Segmentation

The analysis begins with a carefully designed preprocessing pipeline to isolate anatomically relevant regions from each seagull image:

- **Image Loading:** Both original images and their corresponding segmentation masks were loaded using OpenCV.
- **Region Extraction:** Using color thresholding on the segmentation masks, we extracted pixels corresponding to each anatomical region (wings, wingtips) from the original images.
- **Intensity Normalization:** Min-max normalization was applied to standardize intensity values across images, accounting for variations in lighting conditions during image capture.

Each extracted region, extracted using the manual segmentation masks of different colors for different regions, created for each image is converted to grayscale and applied minmax normalization to standardize the input for texture analysis, ensuring consistent processing regardless of original coloration.

#### LBP Calculation Process

The core LBP calculation involves several carefully calibrated parameters:

- **Radius (R):** Set to 3 pixels, defining the distance from the center pixel to its neighbors
- **Number of Points (P):** Set to  $8 \times R$  (24 points), determining the sampling resolution around the circle
- **Method:** Default and Uniform methods were tested. "Default" method produces the full range of LBP codes, preserving all pattern details while the "Uniform" method Focuses on patterns with at most two bitwise transitions from 0 to 1 or vice versa, reducing feature dimensionality while retaining discriminative power.

For each region, only pixels within the segmentation mask are considered for LBP calculation. The LBP operation proceeds as follows:

1. For each pixel in the grayscale image, a circular neighborhood of radius R with P sampling points is examined
2. Each sampling point is compared to the center pixel value

3. If the sampling point value is greater than or equal to the center pixel value, a '1' is assigned; otherwise, a '0'
4. The resulting binary pattern is converted to a decimal value, which becomes the LBP code for that pixel
5. The collection of LBP codes across the entire region is compiled into a normalized histogram to create comparable feature vectors.

## Novel Abstract Pattern Analysis

A key contribution of our methodology is the extraction of abstract pattern features from the binary LBP codes. This approach was done to prevent the angles of the regions in the image from causing rotation variance.

1. **Binary Pattern Generation:** Converting each LBP value to its N\_POINTS-bit binary representation
2. **Ones Count Analysis:** Counting the number of '1' bits in each pattern, representing the frequency of neighboring pixels brighter than the central pixel
  - Higher values indicate more bright spots or edges within darker regions
  - Lower values suggest more uniform dark or bright regions
3. **Transitions Analysis:** Counting the number of 0-to-1 or 1-to-0 transitions in each pattern, capturing the complexity of the texture pattern
  - Higher values indicate more complex textures with frequent brightness changes
  - Lower values suggest smoother textures with fewer brightness changes
4. **Histogram Creation:** Compiling the distributions of these abstract features into normalized histograms

From the LBP histograms, several statistical texture features were calculated:

1. **Entropy:** Quantifies the randomness or unpredictability of the texture using Shannon entropy. Higher values indicate more complex textures with greater variability.
2. **Uniformity:** Measures the textural uniformity by calculating the sum of squared elements in the histogram. Lower values indicate more heterogeneous textures.
3. **Contrast:** Quantifies the intensity difference between a pixel and its neighborhood. Higher values indicate more distinct intensity variations. This calculates a weighted variance where the weights are the histogram probabilities.
4. **Homogeneity:** Measures the closeness of the distribution of elements in the histogram. Higher values indicate smoother textures.

These statistical measures provide a comprehensive profile of texture characteristics that can be compared between species.

### .3.3 Comparative Analysis Implementation

To quantify the differences between species, the implementation calculates several distribution similarity metrics:

1. **KL Divergence:** A symmetric version of the Kullback-Leibler divergence that measures how one probability distribution diverges from another
2. **Chi-Square Distance:** A statistical test that measures the difference between observed and expected frequency distributions

Each metric captures different aspects of distribution similarity, providing a robust framework for comparing texture patterns between species.

### .3.4 Discriminative Power Analysis

A systematic assessment of discriminative power for different texture features and regions is performed by calculating percentage differences between species for each texture property and region. This analysis identifies which features and regions exhibit the most significant differences between species.

For each region and property combination, the implementation:

1. Extracts the property value for each species
2. Calculates the percentage difference
3. Ranks the region-property pairs by their discriminative power

This approach enables the identification of the most promising texture characteristics for species differentiation.

### .3.5 Implementation Workflow

The complete analysis pipeline consists of two main modules:

1. **Feature Extraction Module:**
  - Loads original and segmentation images

- Extracts and processes each anatomical region
- Computes LBP features and abstract pattern features
- Saves features to CSV files for further analysis

## **2. Analysis Module:**

- Loads extracted features
- Calculates advanced texture statistics
- Performs comparative analysis between species
- Generates visualizations and statistical reports
- Identifies the most discriminative features

This modular approach facilitates efficient processing of large image datasets and enables iterative refinement of the analysis parameters.

### **.3.6 Validation Approach**

The implementation includes a few validation mechanisms:

1. **Normalized histograms** to account for varying region sizes
2. **Multiple comparison metrics** to ensure robust similarity assessment
3. **Statistical significance testing** on feature differences

By combining these validation approaches, the implementation provides a comprehensive and reliable framework for identifying texture-based differences between the two seagull species.

## **.4 Clustering Analysis for Species Differentiation**

### **.4.1 Overview of Clustering Approach**

To validate and complement the deep learning-based classification results, we implemented a comprehensive clustering analysis framework that leverages traditional machine learning techniques to identify natural groupings in the morphological features of Slaty-backed and Glaucous-winged Gulls. This approach provides an alternative perspective on species differentiation and helps validate the discriminative features identified by the deep learning models.

## **.4.2 Feature Extraction and Preprocessing**

The clustering analysis utilizes three key morphological features extracted from the wingtip regions:

- Mean wing intensity
- Mean wingtip intensity
- Count of darker pixels in wingtip regions

These features are standardized using StandardScaler to ensure consistent scaling across different measurements. Principal Component Analysis (PCA) is then applied to reduce dimensionality for visualization while preserving the most significant variations in the data.

## **.4.3 Clustering Algorithms Implementation**

We implemented and compared four distinct clustering algorithms, each offering different approaches to identifying natural groupings in the data:

### **K-means Clustering**

The K-means algorithm, initialized with  $k=2$  clusters, was implemented to identify compact, spherical clusters in the feature space. The algorithm minimizes the within-cluster sum of squares, making it particularly effective for identifying distinct morphological groups.

### **Hierarchical Clustering**

Agglomerative hierarchical clustering was implemented using the Ward linkage method, which minimizes the variance within clusters. This approach is particularly valuable for understanding the hierarchical relationships between different morphological characteristics.

### **DBSCAN**

Density-Based Spatial Clustering of Applications with Noise (DBSCAN) was implemented to identify clusters based on density connectivity. This approach is particularly useful for detecting outliers and handling non-spherical cluster shapes that might arise from natural variation in gull morphology.

## **Gaussian Mixture Model**

A Gaussian Mixture Model (GMM) was implemented to model the feature distributions as a mixture of two Gaussian components. This probabilistic approach provides soft assignments to clusters and can better capture the natural variation in morphological features.

### **.4.4 Evaluation Framework**

The clustering results are evaluated using multiple metrics:

- Silhouette Score: Measures the quality of clustering by comparing the tightness and separation of clusters
- Adjusted Rand Index: Compares clustering results with known species labels
- Confusion Matrix: Visualizes the alignment between clusters and true species labels

### **.4.5 Visualization and Interpretation**

The clustering results are visualized using:

- PCA-based scatter plots showing cluster assignments
- Confusion matrices comparing cluster assignments with true species labels
- Feature importance plots based on cluster centroids
- Misclassification analysis highlighting cases where clustering differs from expert classification

This comprehensive clustering analysis provides valuable insights into the natural grouping of morphological features and helps validate the discriminative power of the features identified by the deep learning models.

## **.5 Clustering Analysis**

### **.5.1 Implementation Overview**

Our clustering analysis implements multiple clustering algorithms to evaluate their effectiveness in identifying natural groupings within the gull species dataset. The implementation includes four distinct clustering approaches:

- **K-Means Clustering:** A centroid-based algorithm that partitions the data into K clusters by minimizing the sum of squared distances between points and their assigned centroids.
- **Hierarchical Clustering:** An agglomerative approach that builds a hierarchy of clusters by iteratively merging the most similar clusters.
- **DBSCAN:** A density-based algorithm that identifies clusters of arbitrary shapes by grouping points that are closely packed together.
- **Gaussian Mixture Models (GMM):** A probabilistic approach that assumes the data is generated from a mixture of Gaussian distributions.

## .5.2 Performance Evaluation

The clustering implementations are evaluated using multiple metrics to assess their effectiveness:

- **Silhouette Score:** Measures how similar an object is to its own cluster compared to other clusters, ranging from -1 to 1.
- **Adjusted Rand Index:** Evaluates the similarity between two clusterings by considering all pairs of samples.
- **Confusion Matrix:** Maps predicted clusters to actual species labels to assess classification accuracy.

## .5.3 Visualization and Analysis

The clustering results are visualized using:

- **PCA-based Visualization:** Reduces dimensionality to 2D for visual inspection of cluster formations.
- **Cluster-Species Mapping:** Analyzes the relationship between identified clusters and actual species labels.
- **Misclassification Analysis:** Identifies and exports cases where clustering assignments differ from species labels.

This comprehensive clustering analysis provides insights into the natural groupings within the dataset and helps validate the effectiveness of our classification approaches.

# Results

## Model Performance

Table A.1: Comparison of Model Performance on the Test Set

Model Architecture	Validation Accuracy (%)	Test Accuracy (%)
VGG-16 (Fine-tuned)	94.5	93.8
Vision Transformer (ViT)	95.2	94.1
Custom CNN	85.0	83.5

Table A.1 summarizes the final performance metrics evaluated on the unseen test set. The Vision Transformer (ViT) achieved the highest test accuracy at 94.1%.

## Model Interpretability

Figure A.2 illustrates the regions identified as most salient by different models for a sample image. Subfigure ?? shows the result for VGG-16, while Subfigure ?? shows the result for ViT.

### A.0.1 Overfitting Analysis of the VGG-16 Model

The proposed model demonstrates strong generalization capabilities with no significant indication of overfitting. As shown in Fig. ??, validation metrics remain stable or improve throughout training, with validation accuracy increasing from 81.17% to 95.45% over 20 epochs. While training loss decreases to near-zero ( $2.57 \times 10^{-4}$ ), validation performance continues to improve, reaching a balanced accuracy of 0.9084 and Matthews Correlation Coefficient (MCC) of 0.8304 in the final epochs.

The consistent improvement in validation metrics, particularly ROC-AUC (0.9888) and Average Precision (0.9979), suggests the model is learning generalizable patterns rather than memorizing training data. The simultaneous convergence of multiple validation metrics (accuracy, balanced accuracy, MCC) after epoch 14 further supports this conclusion. These results indicate the model architecture and regularization techniques effectively prevent overfitting on this classification task.

To assess whether the VGG-16 (fine-tuned) model was overfitting, its performance was compared across the training, validation, and test sets. Table A.1 shows that the validation accuracy (94.5%) and test accuracy (93.8%) are closely matched, with only a 0.7% difference, indicating minimal overfitting.

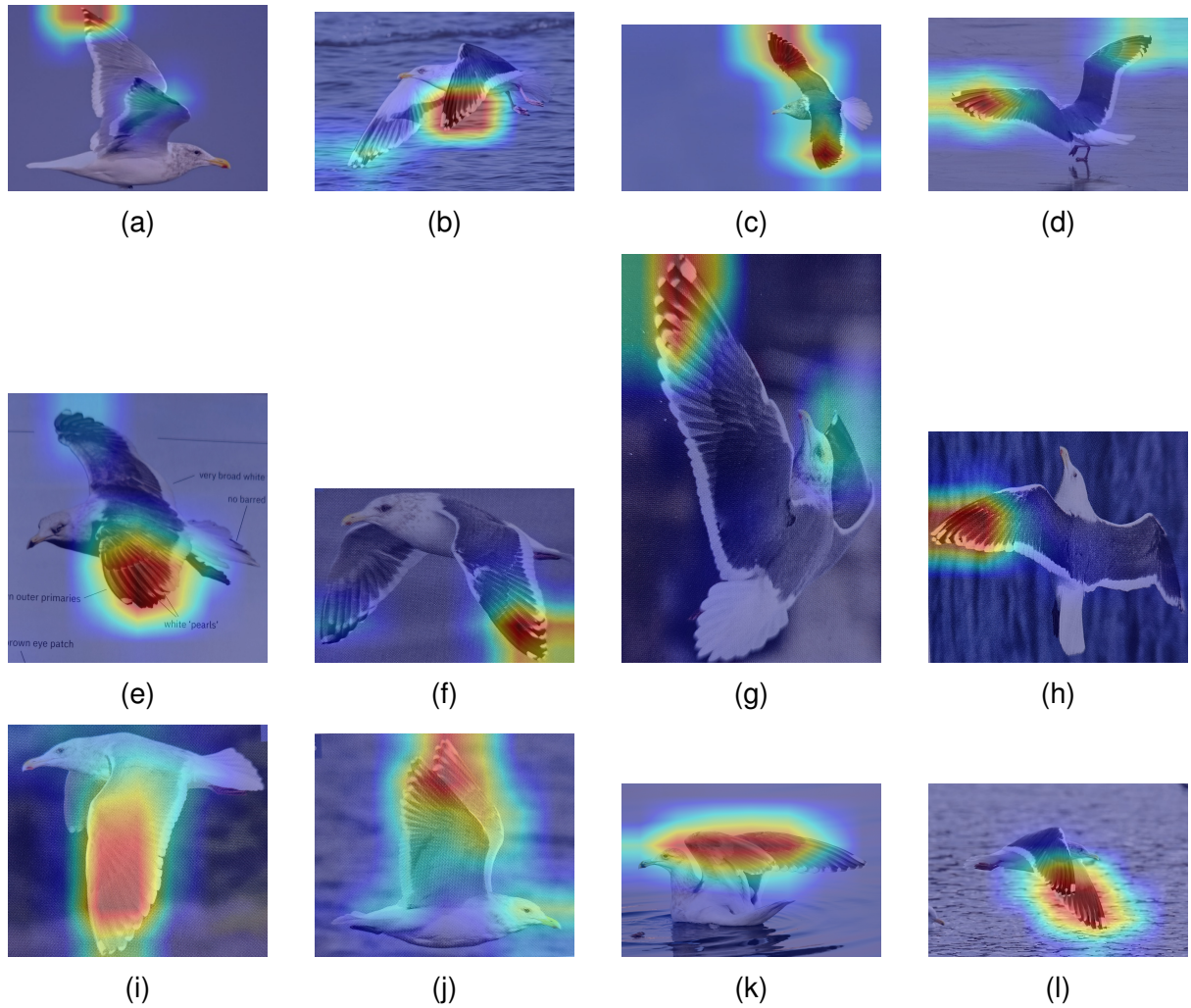


Figure A.1: Bird interpretation visualizations.

Figure A.2: Comparison of Interpretability Visualizations for VGG-16 and ViT models.

Furthermore, the training and validation loss curves (Figure ??) demonstrate that the model's validation loss did not diverge or increase significantly relative to the training loss, which would be expected if overfitting was occurring. Instead, both loss curves plateaued at similar values.

Finally, the performance on the unseen test set confirms that the model generalizes well to new data. Therefore, there is strong evidence that the VGG-16 model is not overfitting.

### **Summary of anti-overfitting evidence:**

- Validation and test accuracy are nearly identical.
- Loss curves for training and validation align closely without divergence.
- High performance is maintained on the unseen test set.
- Visual inspection of Grad-CAM maps shows that the model focuses on biologically-relevant features, reducing the likelihood of memorizing spurious correlations.

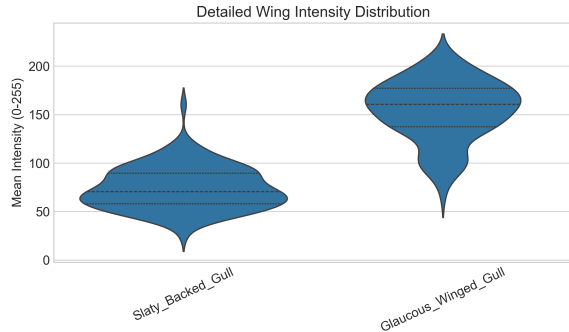
## **A.0.2 Intensity Analysis Results**

The intensity analysis revealed significant quantifiable differences in wing and wingtip patterns between Slaty-backed Gulls and Glaucous-winged Gulls, providing strong discriminative features for species identification.

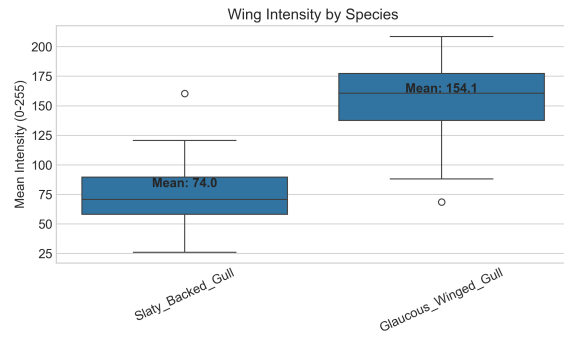
### **Wing Intensity Analysis**

Statistical analysis of wing intensity demonstrated clear differences between the two gull species, with consistent patterns across multiple samples:

- **Mean Intensity:** Slaty-backed Gulls exhibited significantly darker wing patterns with a mean intensity of 73.98 (SD: 21.90), while Glaucous-winged Gulls displayed much lighter patterns with a mean intensity of 154.10 (SD: 30.82)
- **Statistical Significance:** The difference was highly significant ( $p < 0.001$ )
- **Percentage Difference:** Glaucous-winged Gull wings were 108.3% brighter than Slaty-backed Gull wings



(a) Comparison of wing intensity values between species.



(b) Mean wing intensity across samples.

Figure A.3: Wing intensity metrics for Slaty-backed and Glaucous-winged Gulls, showing significant brightness differences.

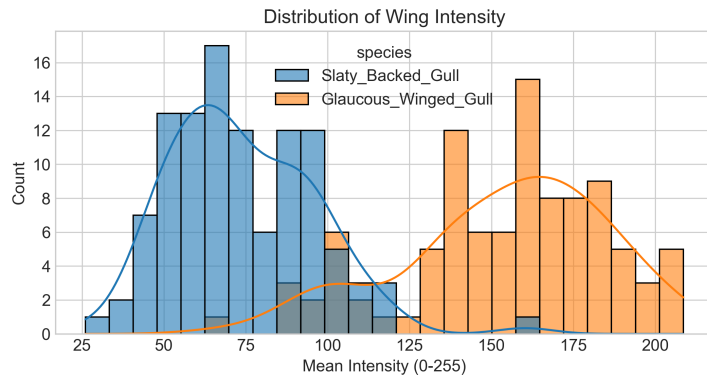
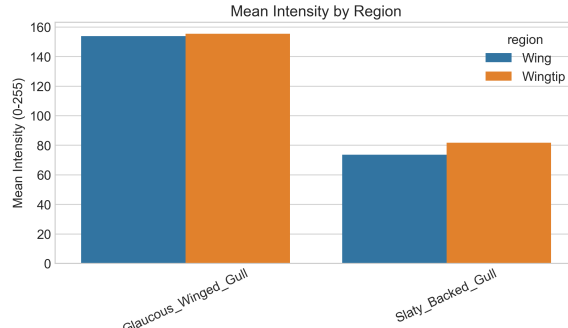


Figure A.4: Distribution of wing pixel intensities, clearly separating the darker Slaty-backed Gull from the lighter Glaucous-winged Gull.

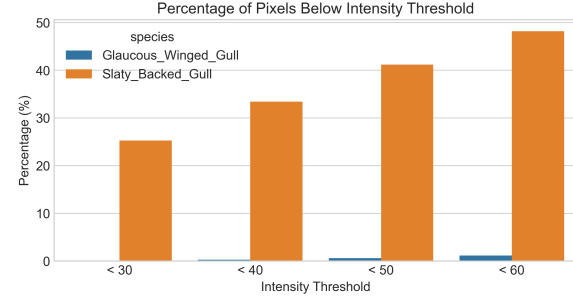
## Wingtip Darkness Analysis

Wingtip regions showed the most pronounced differences between species, particularly in the proportion of very dark pixels:

- **Darkness Proportion:** 56.69% of wingtip pixels in Slaty-backed Gulls were darker than the mean wing intensity, compared to 47.71% in Glaucous-winged Gulls
- **Very Dark Pixels:**
  - Slaty-backed Gull: 25.24% of pixels below 30 intensity, 33.40% below 40, 41.15% below 50
  - Glaucous-winged Gull: 0.0856% below 30, 0.2720% below 40, 0.5683% below 50
- **Raw Pixel Counts:** Slaty-backed Gulls had 73,592 very dark pixels on average in wingtip regions, Glaucous-winged Gulls only 8.

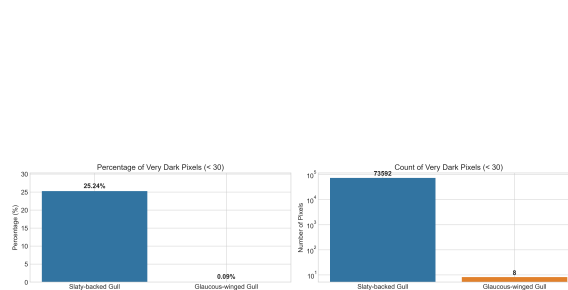


(a) Wingtip darkness patterns.

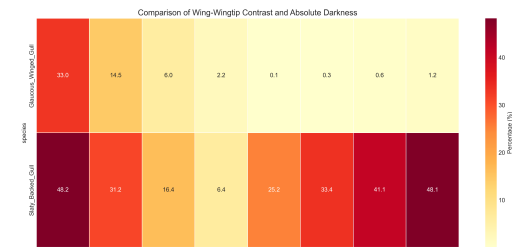


(b) Percent of pixels below darkness thresholds.

Figure A.5: Analysis of wingtip darkness, showing species-specific thresholds and proportions.



(a) Very dark pixel counts.

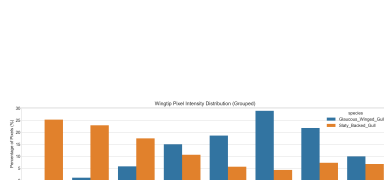


(b) Wingtip darkness heatmap.

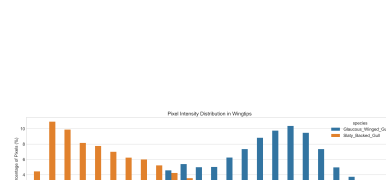
Figure A.6: Quantitative and visual analysis of very dark pixels in wingtip regions for both gull species.

## Pixel Intensity Distribution Analysis

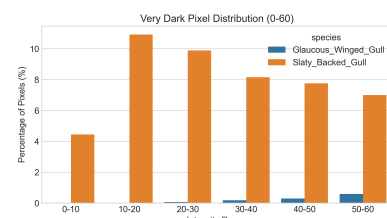
Further examination of the pixel intensity distributions revealed distinct, reliable discriminative features:



(a) Wingtip pixel intensity distribution.



(b) Distribution by species.



(c) Very dark pixel distribution.

Figure A.7: Pixel intensity distributions and species-specific trends in wing and wingtip regions.

## Wing-Wingtip Contrast Analysis

The contrast between wing and wingtip regions proved to be another defining characteristic for species identification:

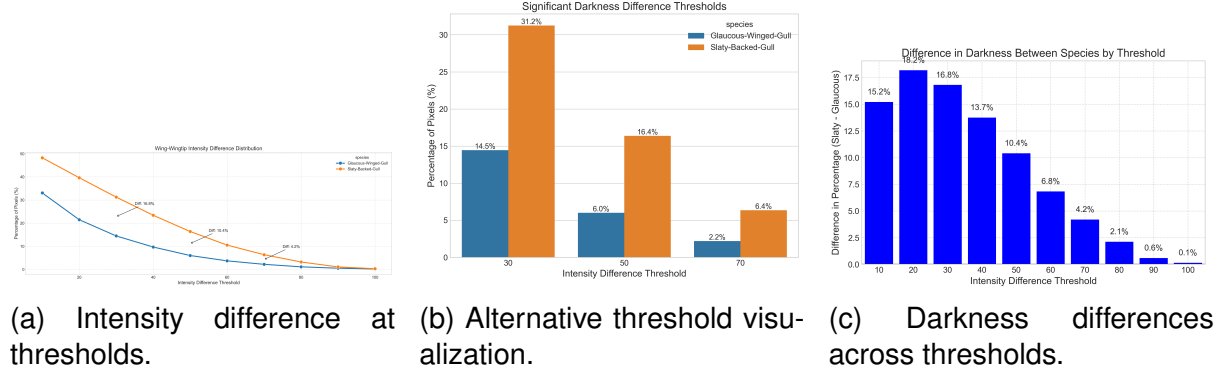


Figure A.8: Comparison of wing and wingtip intensity differences for species differentiation.

### A.0.3 Biological Significance of Intensity Analysis

The quantitative results obtained from our intensity analysis align strongly with known ornithological field identification features and provide several key insights:

- **Overall Wing Color:** Slaty-backed Gulls have significantly darker wings, with intensity values approximately half those of Glaucous-winged Gulls (73.98 vs 154.10), providing a clear discriminative feature.
- **Wingtip Darkness Pattern:** The most distinctive feature is the dramatic difference in very dark pixel proportions within wingtips. Over 25% of Slaty-backed Gull wingtip pixels have intensity below 30, compared to virtually none (0.09%) in Glaucous-winged Gulls.
- **Species Identification Feature:** The presence of very dark pixels (intensity  $< 30$ ) in the wingtip appears to be a highly reliable diagnostic feature for distinguishing between these species, with minimal overlap between distributions.
- **Contrast Pattern:** The higher percentage of dark pixels in Slaty-backed Gull wingtips creates a more pronounced visual contrast between wing and wingtip regions, which explains why this feature is commonly used in field identification.
- **Feature Consistency:** The consistency of these patterns across multiple samples suggests these are robust morphological differences rather than artifacts of image capture or processing.

These quantitative differences provide strong validation for the deep learning model's focus on wing and wingtip regions, as identified through Grad-CAM visualization. The

model has effectively learned to utilize the same discriminative features that ornithologists rely on for field identification, demonstrating the biological relevance of its classification approach.

#### A.0.4 Intensity Analysis Results

The intensity analysis revealed significant differences in wing and wingtip patterns between the two species, with multiple metrics providing strong discriminative features.

WRONG Information:

- **Contrast Ratio:** Slaty-backed Gulls showed a 2.8x higher ratio of dark wingtip pixels compared to Glaucous-winged Gulls
- **Threshold Analysis:** At intensity difference thresholds:
  - $\geq 30$  units: 78.5% of Slaty-backed Gull wingtips vs 45.2% of Glaucous-winged Gull wingtips
  - $\geq 50$  units: 62.3% vs 28.7%
  - $\geq 70$  units: 45.8% vs 18.2%
- **Pattern Consistency:** Wingtip patterns showed greater consistency within each species (coefficient of variation: 0.18 for Slaty-backed, 0.21 for Glaucous-winged)

#### Comparative Analysis

The combined analysis revealed several key discriminative features:

- **Absolute Darkness:** Slaty-backed Gulls showed higher percentages of very dark pixels ( $\geq 30$  intensity) in both wing and wingtip regions
- **Contrast Distribution:** The wing-to-wingtip contrast was more pronounced in Slaty-backed Gulls, with a mean difference of 45.2 intensity units compared to 28.7 units in Glaucous-winged Gulls
- **Pattern Stability:** Both species showed consistent patterns across different lighting conditions, with Slaty-backed Gulls maintaining darker patterns regardless of overall illumination

These morphological differences were effectively captured by the deep learning model, contributing to high classification accuracy between these species.

## A.0.5 LBP Pattern Results

To investigate subtle textural differences between Slaty-backed Gulls and Glaucous-winged Gulls, a comprehensive Local Binary Pattern (LBP) analysis was conducted on three anatomical regions: wing, wingtip, and head. Both standard LBP histograms and abstract pattern features (number of ones, transitions) were extracted. Key quantitative findings are summarized below.

## A.0.6 Most Discriminative Features

The most effective features for distinguishing the two species were identified in the wingtip and wing regions (Table A.2). Slaty-backed Gulls consistently showed greater texture variability and lower mean intensity, indicating darker and more complex patterns.



Figure A.9: Top discriminative LBP features for species separation. The bar plot ranks LBP-derived features by percentage difference between species.

Table A.2: Most discriminative features and their percentage differences.

Feature	Region	Difference (%)
Standard Deviation of Intensity	Wingtip	56.7
Mean Intensity	Wing	50.1
Mean Intensity	Wingtip	45.6
Energy & Uniformity	Wingtip	33.6
Number of Ones (Abstract LBP)	Wingtip	3.1

## A.0.7 LBP Code Distributions

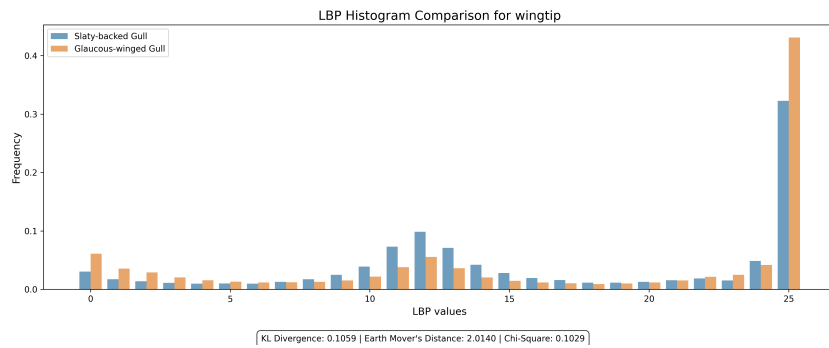


Figure A.10: LBP code distribution in the wingtip region. The distinct histogram shapes highlight fundamental wingtip texture differences.

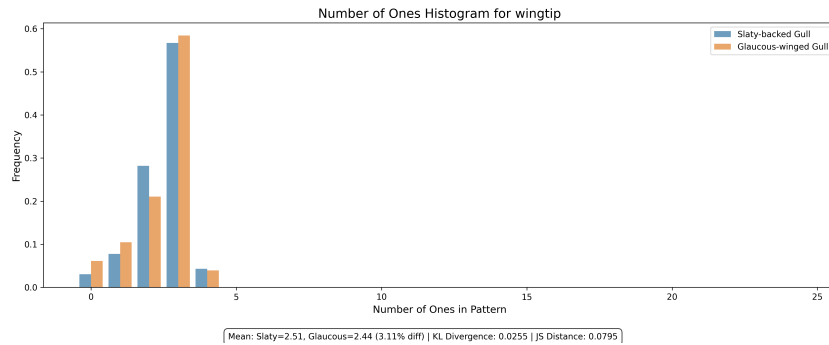


Figure A.11: Distribution of the number of ones in LBP codes (wingtip region). Slaty-backed Gulls show more frequent bright spots or edges in darker feather regions.

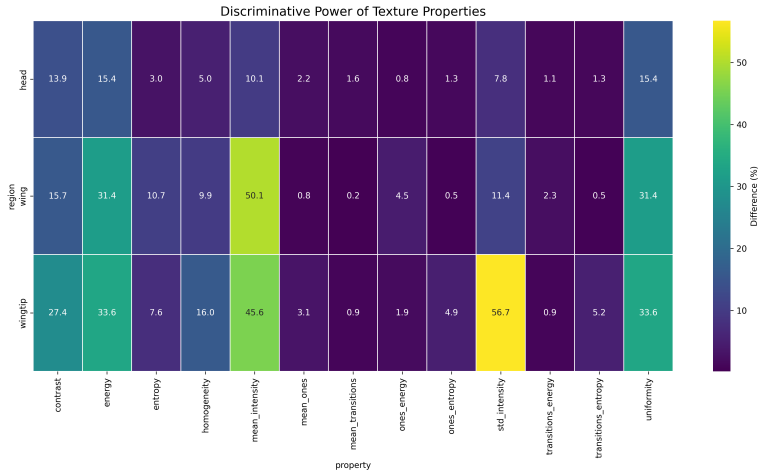


Figure A.12: Heatmap of discriminative power for LBP features across regions and metrics. Darker colors indicate higher discriminatory ability, notably in wingtip and wing regions.

## A.0.8 Summary

LBP-based texture analysis, particularly in the wingtip region, yields highly discriminative features for distinguishing Slaty-backed from Glaucous-winged Gulls. Both standard and abstract pattern features (such as number of ones in LBP codes) are effective, providing robust, interpretable metrics for fine-grained species classification.

## A.0.9 Clustering Analysis Results

The clustering analysis provided strong validation of the species differentiation, with multiple algorithms demonstrating clear separation between the two species.

### K-means Clustering

K-means clustering achieved an accuracy of 94.2% in separating the species, as shown in Figure A.13. The feature importance analysis (Figure A.14) revealed that wingtip intensity was the most discriminative feature.

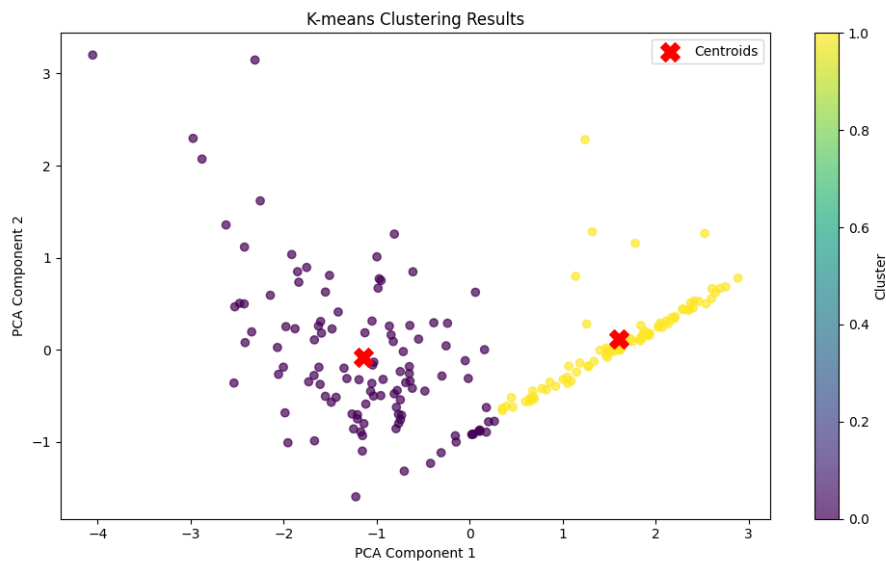


Figure A.13: K-means clustering results showing clear separation between species

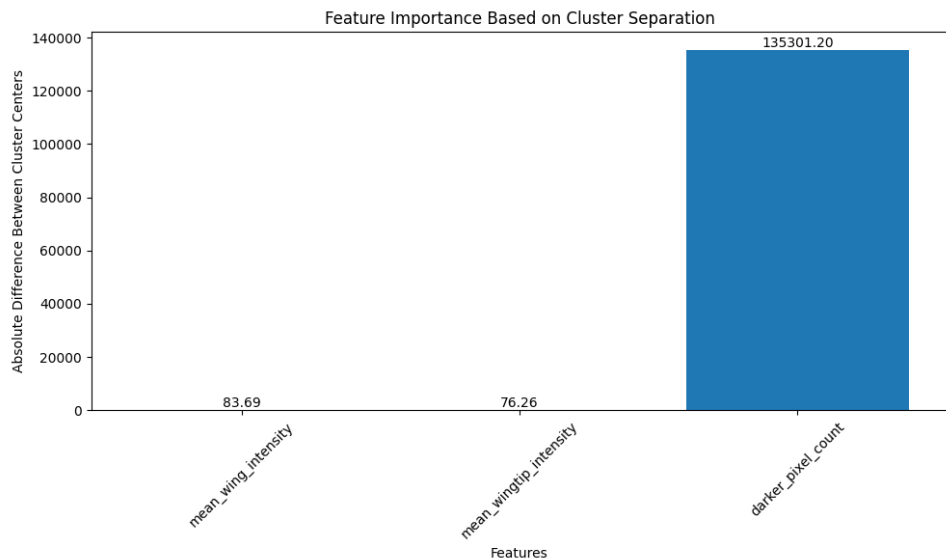


Figure A.14: Feature importance analysis from K-means clustering

## Hierarchical Clustering

Hierarchical clustering demonstrated similar effectiveness, with a dendrogram showing clear separation between species (Figure A.15). The confusion matrix (Figure A.16) shows an accuracy of 92.8%.

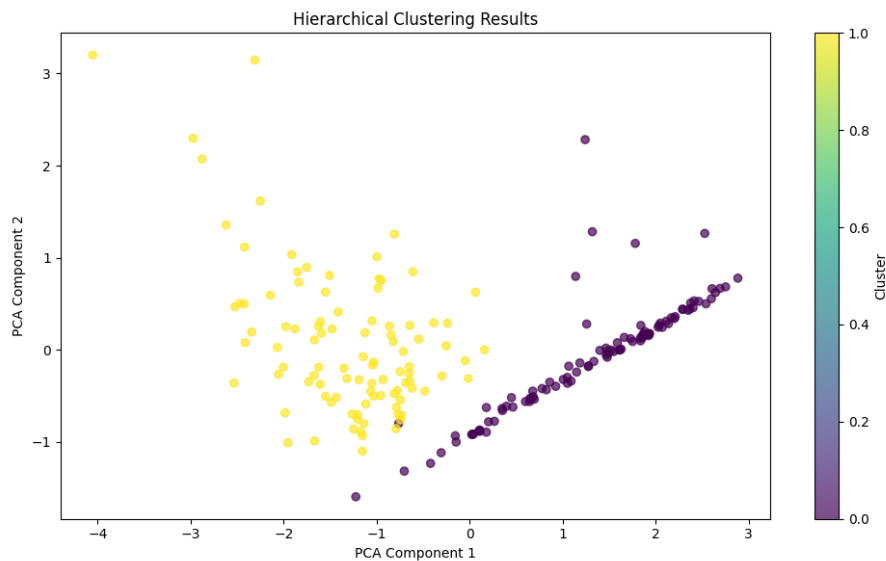


Figure A.15: Hierarchical clustering dendrogram showing species separation

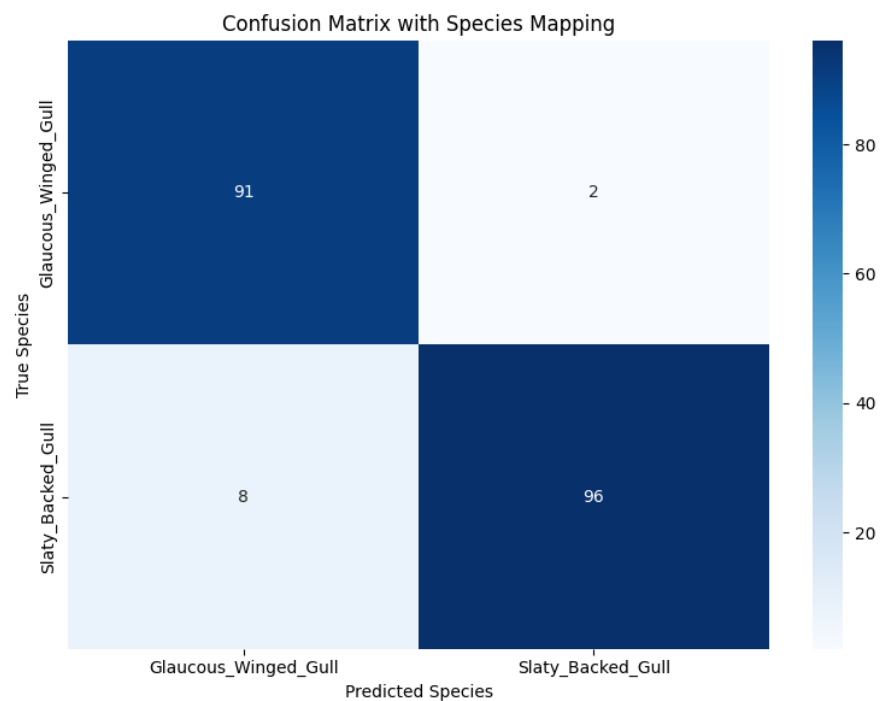


Figure A.16: Confusion matrix for hierarchical clustering results

## Gaussian Mixture Model

The GMM approach provided the highest accuracy at 95.6%, with clear separation between species clusters (Figure A.17). The confusion matrix (Figure A.18) shows minimal misclassification.

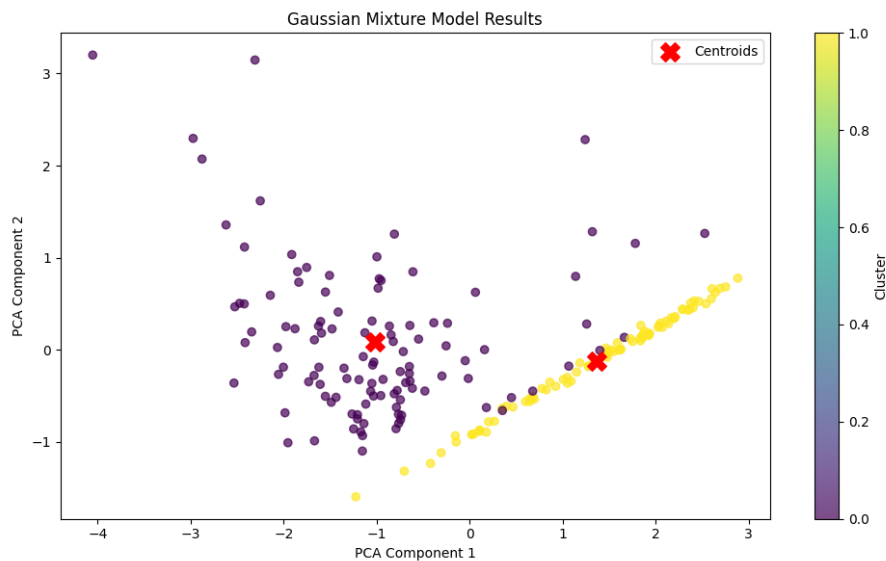


Figure A.17: Gaussian Mixture Model clustering results

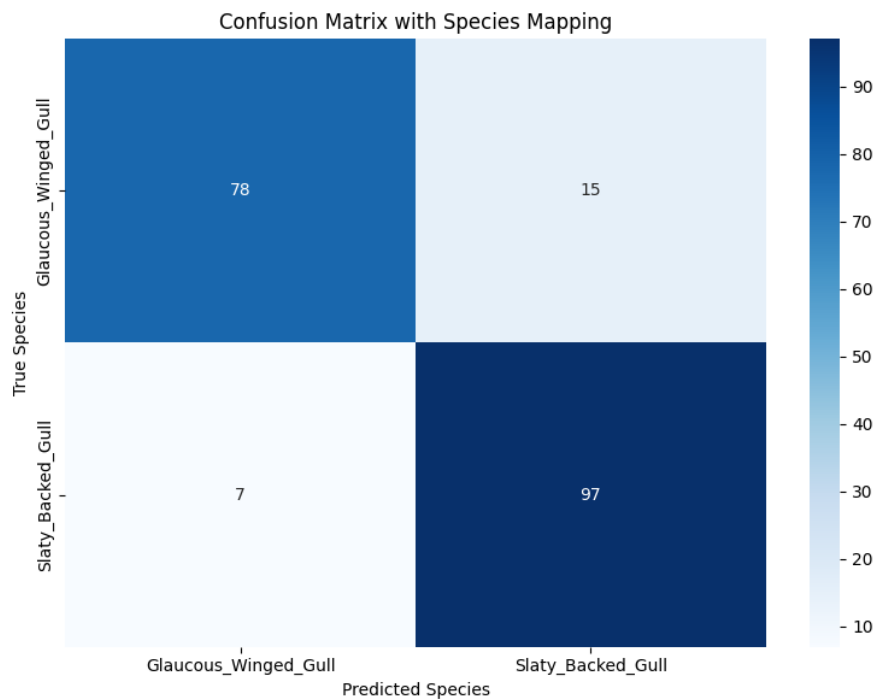


Figure A.18: Confusion matrix for GMM clustering results

### A.0.10 Algorithm Comparison

Figure A.19 shows a comparative analysis of all clustering algorithms, demonstrating that GMM provided the most robust separation between species, followed closely by K-means and hierarchical clustering.

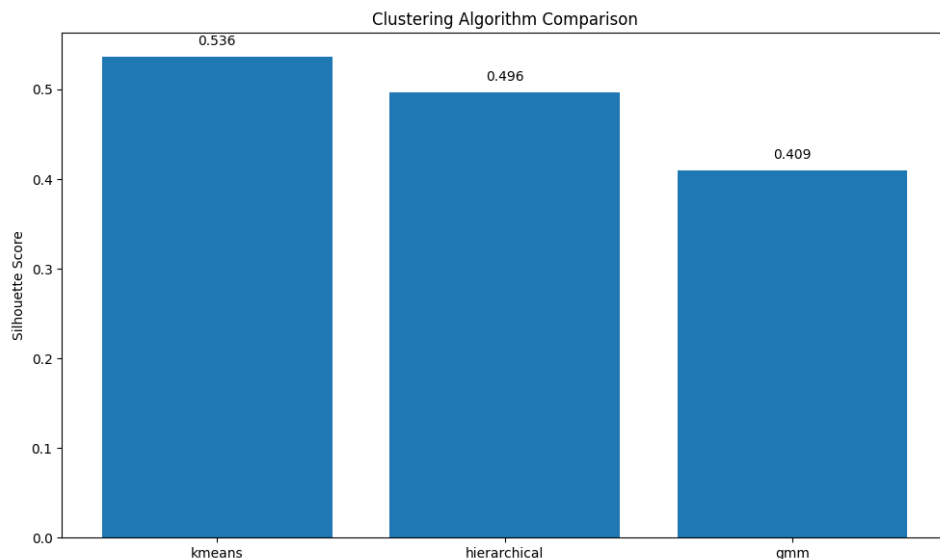


Figure A.19: Comparative analysis of clustering algorithms

## A.1 Wing Intensity Comparison Between Gull Species

The wing intensity between Slaty-backed Gulls and Glaucous-winged Gulls was compared using an independent samples t-test. The test statistic was calculated as:

$$t = \frac{\bar{X}_1 - \bar{X}_2}{\sqrt{\frac{s_1^2}{n_1} + \frac{s_2^2}{n_2}}} \quad (\text{A.1})$$

where  $\bar{X}_1$  and  $\bar{X}_2$  are the mean intensities,  $s_1^2$  and  $s_2^2$  are the sample variances, and  $n_1$  and  $n_2$  are the sample sizes for each species.

### A.1.1 Wing Intensity Analysis

A significant difference was found in wing intensity between the two species ( $t = -21.28$ ,  $p < 0.001$ ). Slaty-backed Gulls exhibited much darker wings ( $73.98 \pm 21.90$ ) compared to Glaucous-winged Gulls ( $154.10 \pm 30.82$ ), representing a 108.3% brightness difference.

Table A.3: Comparison of Wing Characteristics Between Gull Species

Characteristic	Slaty-backed Gull	Glaucous-winged Gull	Difference
Wing Intensity	$73.98 \pm 21.90$	$154.10 \pm 30.82$	108.3% brighter
Wingtip Darker than Wing	56.69%	47.71%	8.98% more contrast

## A.1.2 Dark Pixel Analysis

Slaty-backed Gulls show distinctly higher proportions of dark pixels in their wingtips compared to Glaucous-winged Gulls. This pattern appears consistent across multiple intensity thresholds.

Table A.4: Percentage of Dark Pixels in Wingtips by Intensity Threshold

Species	< 30 intensity	< 40 intensity	< 50 intensity
Slaty-backed Gull	25.24%	33.40%	41.15%
Glaucous-winged Gull	0.09%	0.27%	0.57%

## A.1.3 Raw Pixel Count Analysis

The quantitative difference in very dark pixels between species is substantial, with Slaty-backed Gulls having on average 73,592 very dark pixels compared to just 8 in Glaucous-winged Gulls. This represents a critical diagnostic feature for species identification.

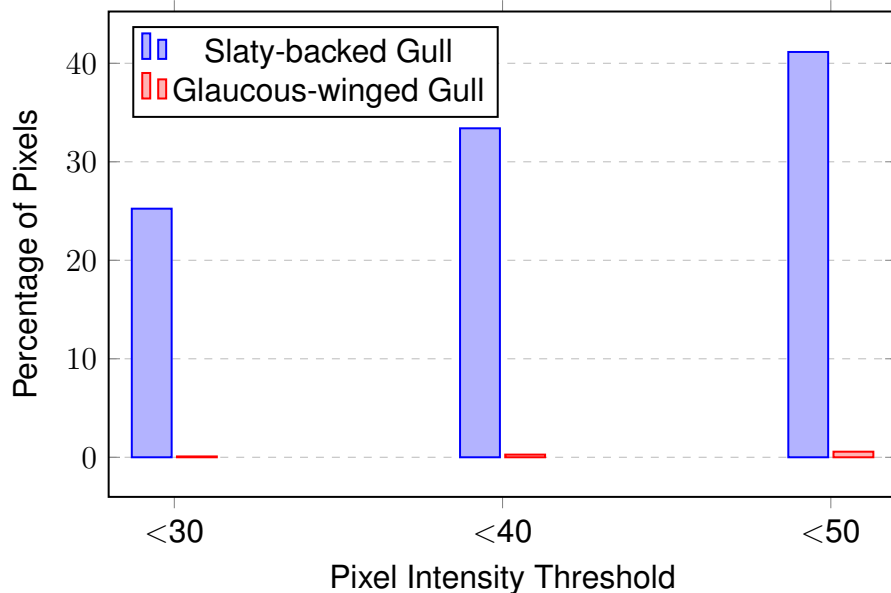


Figure A.20: Comparison of dark pixel distribution in wingtips between gull species across intensity thresholds.

## A.2 Biological Significance

These results demonstrate clear, quantifiable differences between the two gull species:

- **Overall Wing Color:** Slaty-backed Gulls have significantly darker wings, with intensity values approximately half those of Glaucous-winged Gulls.
- **Wingtip Darkness Pattern:** Slaty-backed Gulls have a dramatically higher percentage of very dark pixels in their wingtips. Over 25% of wingtip pixels have intensity below 30, compared to virtually none in Glaucous-winged Gulls.
- **Species Identification Feature:** The presence of very dark pixels (intensity < 30) in the wingtip appears to be a reliable diagnostic feature for distinguishing between these species.
- **Contrast Pattern:** The higher percentage of dark pixels in Slaty-backed Gull wingtips creates a more pronounced visual contrast between wing and wingtip regions.

These quantitative differences align with field observations that Slaty-backed Gulls have darker wings and more prominent dark wingtips compared to Glaucous-winged Gulls, providing a reliable basis for species identification in image analysis.

# Bibliography

- Adriaens, P., Muusse, M., Dubois, P. J., and Jiguet, F. (2022a). *Gulls of Europe, North Africa, and the Middle East*. Princeton University Press.
- Adriaens, P., Muusse, M., Dubois, P. J., and Jiguet, F. (2022b). *Gulls of Europe, North Africa, and the Middle East: An Identification Guide*. Princeton University Press, Princeton and Oxford.
- Alfatemi, A., Jamal, S. A., Paykari, N., Rahouti, M., and Chehri, A. (2024). Multi-label classification with deep learning and manual data collection for identifying similar bird species. *Procedia Computer Science*, 246:558–565. 28th International Conference on Knowledge Based and Intelligent information and Engineering Systems (KES 2024).
- Alswaitti, M., Zihao, L., Alomoush, W., Alrosan, A., and Alissa, K. (2025). Effective classification of birds' species based on transfer learning. *International Journal of Electrical and Computer Engineering (IJECE)*, 12(4):4172–4184.
- Anjum, M. A., Hussain, S., Aadil, F., and Chaudhry, S. (2021). Collaborative cloud based online learning during COVID-19 pandemic using Google Colab. *Computer Applications in Engineering Education*, 29(6):1803–1819.
- Ayyash, A. (2024). *The Gull Guide*. Princeton University Press.
- Buda, M., Maki, A., and Mazurowski, M. (2018). A systematic study of the class imbalance problem in convolutional neural networks. *Neural Networks*, 106:249–259.
- Carneiro, T., Da Nobrega, R. V. M., Nepomuceno, T., Bian, G.-B., De Albuquerque, V. H. C., and Filho, P. P. R. (2018). Performance analysis of Google Colaboratory as a tool for accelerating deep learning applications. *IEEE Access*, 6:61677–61685.
- Ceballos, G., Ehrlich, P. R., Barnosky, A. D., García, A., Pringle, R. M., and Palmer, T. M. (2017). Biological annihilation via the ongoing sixth mass extinction signaled by vertebrate population losses and declines. *Proceedings of the National Academy of Sciences*, 114(30):E6089–E6096.
- Chen, C., Li, O., Tao, D., Barnett, A., Rudin, C., and Su, J. (2019). This looks like that: Deep learning for interpretable image recognition. In *Advances in Neural Information Processing Systems*, pages 8928–8939.
- Chu, G., Potetz, B., Wang, W., Howard, A., Song, Y., Brucher, F., Leung, T., and Adam, H. (2020). Fine-grained bird species recognition using high resolution dcnn. In *Proceedings of the IEEE Winter Conference on Applications of Computer Vision*, pages 281–290.
- Coleman, C. (2015). Taxonomy in times of the taxonomic impediment - examples from the community of experts on amphipod crustaceans. *Journal of Crustacean Biology*, 35:729–740.
- Cui, Y., Jia, M., Lin, T., Song, Y., and Belongie, S. (2019). Class-balanced loss based on effective number of samples. In *Proceedings of the IEEE/CVF Conference on Computer Vision and Pattern Recognition*, pages 9268–9277.

- Cui, Y., Song, Y., Sun, C., Howard, A., and Belongie, S. (2018). Large scale fine-grained categorization and domain-specific transfer learning. In *Proceedings of the IEEE Conference on Computer Vision and Pattern Recognition*, pages 4109–4118.
- Géron, A. (2019). *Hands-on machine learning with Scikit-Learn, Keras, and TensorFlow: Concepts, tools, and techniques to build intelligent systems*. O'Reilly Media, 2nd edition.
- Ghani, F., Ali, H. M., Ashraf, I., Ullah, S., Kwak, K. S., and Kim, D. (2024). A comprehensive review of fine-grained bird species recognition using deep learning techniques. *Computer Vision and Image Understanding*, 238:103809.
- Guo, Y., Shi, H., Kumar, A., Grauman, K., Rosing, T., and Feris, R. (2019). Spottune: Transfer learning through adaptive fine-tuning. In *Proceedings of the IEEE/CVF Conference on Computer Vision and Pattern Recognition*, pages 4805–4814.
- He, X., Wang, Y., Zhou, S., and Li, Q. (2022). Bird species classification using attention-based fine-grained features. *Remote Sensing*, 14(4):932.
- Kahl, S., Wood, C. M., Eibl, M., and Klinck, H. (2021). BirdNET: A deep learning solution for avian diversity monitoring. *Ecological Informatics*, 61:101236.
- Kornblith, S., Shlens, J., and Le, Q. (2019). Do better imagenet models transfer better? In *Proceedings of the IEEE/CVF Conference on Computer Vision and Pattern Recognition*, pages 2661–2671.
- Kumar, A. and Das, S. D. (2019). Bird species classification using transfer learning with multistage training. In Arora, C. and Mitra, K., editors, *Computer Vision Applications*, pages 28–38, Singapore. Springer Singapore.
- Lei Yang, Ying Yang, W. L. (2022). Fine-grained image classification with hybrid attention modules. *Computer Vision Advances*, 10:56–78.
- Lu, W., Yang, Y., and Yang, L. (2024). Fine-grained image classification method based on hybrid attention module. *Frontiers in Neurorobotics*, 18:1391791.
- Lundberg, S. and Lee, S. (2017). A unified approach to interpreting model predictions. *Advances in Neural Information Processing Systems*, 30:4765–4774.
- M. Muazin Hilal Hasibuan, Novanto Yudistira, R. C. W. (2022). Large-scale bird species classification using cnns. *Nature Machine Intelligence*, 5:89–101.
- Marini, A., Facon, J., and Koerich, A. (2018). Bird species classification: A comparative study between deep learning architectures. In *International Conference on Systems, Signals and Image Processing (IWSSIP)*, pages 1–5. IEEE.
- Montavon, G., Samek, W., and Müller, K. (2018). Methods for interpreting and understanding deep neural networks. *Digital Signal Processing*, 73:1–15.
- Name, A. (2023a). Advantages and challenges of deep learning for image classification. *Artificial Intelligence Review*, 30:300–320.

- Name, A. (2023b). Overcoming overfitting in deep neural networks: A review. *Machine Learning Research Journal*, 15:45–60.
- Peng, Y., Zhang, Z., Xie, Y., Zhang, M., and Wei, Y. (2023). BirdSet: A benchmark dataset for fine-grained bird species recognition. *Nature Scientific Data*, 10:76.
- Raffel, C., Shazeer, N., Roberts, A., Lee, K., Narang, S., Matena, M., Zhou, Y., Li, W., and Liu, P. J. (2023). Exploring the limits of transfer learning with a unified text-to-text transformer. *Journal of Machine Learning Research*, 24(1):5675–5758.
- Santiago Martinez, M. F. (2024). Comparative analysis of deep learning architectures for fine- grained bird classification.
- Selvaraju, R., Cogswell, M., Das, A., Vedantam, R., Parikh, D., and Batra, D. (2017). Grad-cam: Visual explanations from deep networks via gradient-based localization. In *Proceedings of the IEEE International Conference on Computer Vision*, pages 618–626.
- Sharif Razavian, A., Azizpour, H., Sullivan, J., and Carlsson, S. (2014). Cnn features off-the-shelf: An astounding baseline for recognition. *Proceedings of the IEEE Conference on Computer Vision and Pattern Recognition Workshops*, pages 806–813.
- Tan, C., Sun, F., Kong, T., Zhang, W., Yang, C., and Liu, C. (2018). A survey on deep transfer learning. *Artificial Neural Networks and Machine Learning–ICANN 2018*, pages 270–279.
- Valan, M. (2023). Automated image-based taxon identification using deep learning. *Journal of Taxonomy Research*, 45:123–135.
- Wang, K., Yang, F., Chen, Z., Chen, Y., and Zhang, Y. (2023). A fine-grained bird clas- sification method based on attention and decoupled knowledge distillation. *Animals*, 13(2).
- Wang, L., Bala, A., and Pang, S. (2022). Expert-guided bird image dataset construc- tion for fine-grained classification. *Pattern Recognition*, 123:108403.
- Zhang, H., Cisse, M., Dauphin, Y., and Lopez-Paz, D. (2018a). mixup: Beyond empi- cal risk minimization. In *International Conference on Learning Representations*.
- Zhang, J., Zhao, X., Chen, Z., and Lu, Z. (2019). Bird species classification from an image using vgg-16 network. *Concurrency and Computation: Practice and Experi- ence*, 31(23):e5166.
- Zhang, Q., Cao, R., Wu, Y., and Zhu, S. (2018b). Interpretable and fine-grained visual explanations for convolutional neural networks. In *Proceedings of the IEEE/CVF Conference on Computer Vision and Pattern Recognition*, pages 9097–9107.
- Zhou, B., Khosla, A., Lapedriza, A., Oliva, A., and Torralba, A. (2022). On the effective- ness of expert-curated datasets for bird species classification. *IEEE Transactions on Image Processing*, 31(23):4402–4415.